COPY No. 1

Open File 943

REPORT ON THE COTRAN^R SURVEY CONDUCTED IN THE ATHABASCA BASIN FOR THE GEOLOGICAL SURVEY OF CANADA

INFORMATION

BARRINGER RESEARCH

Copy

REPORT ON THE COTRAN^R SURVEY CONDUCTED IN THE ATHABASCA BASIN FOR THE GEOLOGICAL SURVEY OF CANADA

CONFIDENTIAL INFORMATION
THIS DOCUMENT CONTAINS INFORMATION
PROPRIETARY TO BARRINGER RESEARCH
LIMITED AND SHALL NOT BE REPRODUCED
OR TRANSFERRED TO OTHER DOCUMENTS,
OR DISCLOSED TO OTHERS, OR USED FOR
ANY PURPOSE OTHER THAN THAT FOR
WHICH IT IS FURNISHED WITHOUT THE
PRIOR WRITTEN PERMISSION OF
BARRINGER RESEARCH LIMITED.

PREPARED BY:

Barringer Research Limited
304 Carlingview Drive
Rexdale, Ontario
M9W 5G2

6204A

TABLE OF CONTENTS

BARRINGER RESEARCH

BARRINGER RESEARCH LIMITED
304 CARLINGVIEW DRIVE
METROPOLITAN TORONTO
REXDALE, ONTARIO
CANADA M9W 5G2
PHONE 416-675-3870
TELEX 06-989183

January 19, 1982

Mr. Len Collett
Geological Survey of Canada
601 Booth Street
OTTAWA, Ontario

Dear Mr. Collett:

Further to our recent telephone conversation, I would like to confirm that the technical information contained in the document entitled, "Report on the COTRAN Survey Conducted in the Athabasca Basin for the Geological Survey of Canada", submitted by Barringer Research Limited to the Geological Survey of Canada as a final report on the activities carried out under the DSS Contract #OSQ79-00164 is no longer considered to be of a confidential nature. Subsequently, please consider this letter as a formal permission from BRL to GSC to release the above report for distribution to the public at your discretion.

I would like to point out that the COTRAN system hardware and software, as well as the quality of data, described in the report represent the state-of-the-art in COTRAN technology as it was in 1980. Since that time, substantial improvements have been made in the system hardware, and new, more powerful algorithms and software have been developed for post-time data reduction, which considerably improved the quality of data. These improvements have been thoroughly tested during the past year on four separate test surveys, one of which was of considerable size. Totally, nearly 5000 line miles were flown in Canada and the U.S. in 1981. The results are being evaluated now, and will be reported on in the near future.

I trust the COTRAN system will be commercially available for full production surveys in Canada during this coming 1982 exploration season.

Yours truly,

BARRINGER RESEARCH LIMITED

L. R. Daubner
General Manager, R & D

LRD:ki

ADVANCED T ES AND INSTRUMENTATION FOR THE EARTH SCIENCES

1. INTRODUCTION

This report summarizes the results of the first operational survey carried out with the Barringer COTRAN airborne electromagnetic (AEM) system. The survey was an evaluation study of the COTRAN system sponsored by the Geological Survey of Canada (GSC). The objectives of the survey were twofold. The first objective was to carry out an operational survey to assess the overall performance of the COTRAN system. The second objective was to test the ability of the COTRAN system to detect deep, known conductors.

The survey was carried out in the Athabasca Basin area of Northern Saskatchewan. The COTRAN survey area forms part of the general GSC study area where high sensitivity magnetometer and vertical gradiometer survey programs have been carried out previously. A number of known uranium deposits are located within the test survey area. These unconformity-type uranium deposits are located at the contact between the overlying Athabasca sandstone formation and the Precambrian basement. The deposits are generally associated with extensive graphitic conductors located in the basement. Since the thickness of the overlying Athabasca sandstone varies from 50 to 250 m within the COTRAN survey area, the site provides an ideal area to assess the depth penetration capabilities of an EM system.

This report gives a general overview of the COTRAN AEM system as well as analysis of the survey program and the resulting survey data. Since the COTRAN AEM system is totally new and a marked departure from any previous AEM system, an extensive description of the system concepts as well as its hardware and software implementation are provided in Section 2, 3 and 4 of the report. The system description is followed by a review of the survey area and the operational survey program. An analysis of the reduced EM data is then presented followed by a summary of the overall results obtained with the test survey program.

2. COTRAN PRINCIPLES

The COTRAN (COrrelation of TRANsients) method is a significant departure from the basic techniques used in existing EM systems. In the following, a brief summary of the basic concepts of the COTRAN method is given in order to provide a basis for the description of the hardware implementation and data processing aspects of the COTRAN system.

The basic objective of EM measurements is to ascertain the electrical conductivity of the ground. This measurement is based on the basic laws of electromagnetic induction, namely, Ampere's law and Faraday's law. With active EM systems, a localized time varying primary magnetic field source induces eddy currents to flow in the ground. The magnitude of the eddy current and its spatial extent is a complex function of the source geometry, the ground conductivity and the frequency of excitation. The eddy currents induced to flow in the ground are sensed with electric and magnetic field sensors which detect the secondary electromagnetic fields associated with the eddy currents. The observed secondary fields are then used to infer the spatial distribution of electrical conductivity of the ground in the vicinity of the EM system.

With airborne EM systems, a relatively fixed transmitter-receiver geometry is transported over the ground by a fixed or rotary wing aircraft. In order to maximize the information about ground conductivity, the transmitter must energize the ground over as wide a frequency band as possible. In addition, measurements should be made sufficiently often to assure that the variations in conductivity are adequately resolved when the system is being transported at high speed over the ground. In practice, such measurements must be made in the presence of noise from various sources such as atmospheric noise, aircraft noise, receiver motion in the earth's natural magnetic field and cultural noise from power lines, radio stations, etc.

Without getting into too many details, the EM problem can be viewed in the same manner as a measurement of a system transfer function or impulse response function. With the aid of Fig. 2-1, the field at a receiving sensor is the superposition of the primary field from the transmitter and the secondary field from the ground.

Denoting a particular field component at the receiver position by R, one has

$$R = R_p + R_s + \text{Noise}$$

where R_p is the primary field component and R_s is the secondary field component. R_p and R_s are functions of spatial position and time. Within the quasistatic assumption for low frequency electromagnetic fields in air, one can express R as

$$R\,(t) = A(\bar{r},\ \bar{r}_o)\ P(t) + B(\bar{r},\ \bar{r}_o) \int_0^\infty G(\beta)\ P(t-\beta)\ d\beta\ + N(t)$$

where

$A(\bar{r}, \bar{r}_o)$ = geometrical coupling factor between transmitter and receiver

$B(\bar{r}, \bar{r}_o)$ = geometrical coupling factor between the ground and the transmitter and receiver

$\bar{r}_o$ = position of the transmitter

$\bar{r}$ = position of the receiver

t = time

$P(t)$ = time variation of primary field

$G(t)$ = impulse response function of the ground

$N\,(t)$ = noise

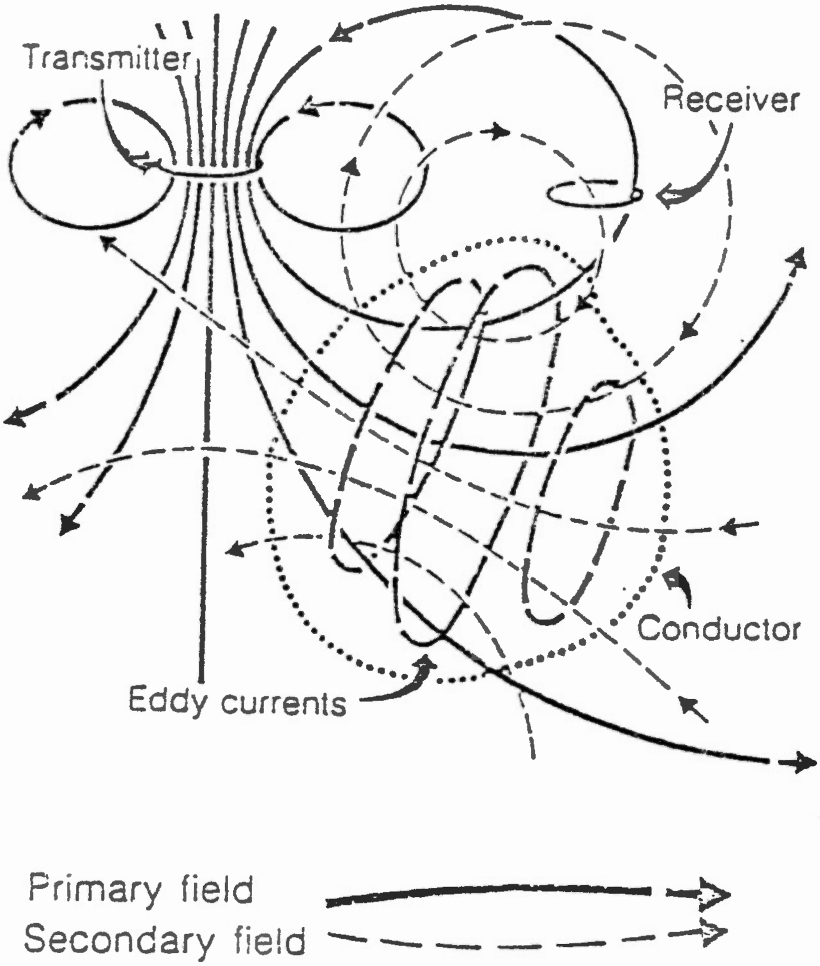
Transmitter
Receiver
Conductor
Eddy currents
Primary field
Secondary field

FIG. 2.1

The decomposition of R into the above form provides the basis of the COTRAN method. While the real problem is somewhat more complex than this formulation indicates, the following discussion of COTRAN is changed only in detail but not in principle by not going into the full complexity. The added complexity comes from the fact that A and B are functions of time. As a result one must treat the modulation effects. Suffice it to say that with adequate design of hardware, A and B are made to vary only slowly with time compared with P(t) such that for short periods of time, A and B can be treated as constant.

The above formulation is best understood by considering the special cases of a single frequency system and a transient system such as INPUT. For a single frequency system, the excitation waveform is sinusoidal. By setting

$$P(t) = e^{iwt}$$

R(t) reduces to

$$R(t) = Ae^{iwt} + (I + iQ)e^{iwt} + N(t)$$

with

$$I + iQ = \int_0^\infty G(\beta) e^{-i\omega\beta} d\beta$$

where I and Q are the in-phase and quadrature components of the ground response at frequency W. The main difficulty with single frequency systems is the problem in resolving variations in A, the amplitude of the primary field, from variations in I, the in-phase ground response. Since A is often orders of magnitude larger than I, this is not a trivial problem. For towed bird systems operating in this manner, normally no attempt is made to determine I and only quadrature signals are measured.

With a transient system such as INPUT, an alternative approach is applied. In this case P(t) the primary field is turned on and off and the ground response is measured during the time P(t) is zero. With INPUT, for example, the primary magnetic field has the form

$$
\begin{aligned}
P(t) &= \sin \pi (t/T) && o < t < T \\
&= o && T \leq t < V \\
&= -\sin \pi (t/T) && V \leq t < V+T \\
&= o && V+T \leq t < 2V
\end{aligned}
$$

for each transmit cycle. During the time when P(t) is zero.

$$R(t) = B(r, ro) \int_{o}^{\infty} G(\beta)\ P(t-\beta)\, d\beta \quad + N(t)$$

Measurements of R(t) during the transmitter off times provides a direct measure of ground response provided the ground response is of a form to generate a response when the transmitter is off. The ground fails to produce a significant off-time response for very high or very low conductivity situations. The upper and lower bounds are a function of P(t) and the manner in which R(t) is measured.

Fig. 2-2 schematically illustrates the general behaviour of the ground response. The upper figure depicts the ground transfer function in-phase and quadrature components as a function of frequency. The lower figure depicts the impulse response function of the ground. The ground response behaves in the same manner as a high pass filter. In fact the simple loop response discussed later is identical in form to a first order high pass filter with its 3 dB point at a frequency $f = 1/2\pi\tau$ where τ is the time constant of the loop eddy current.

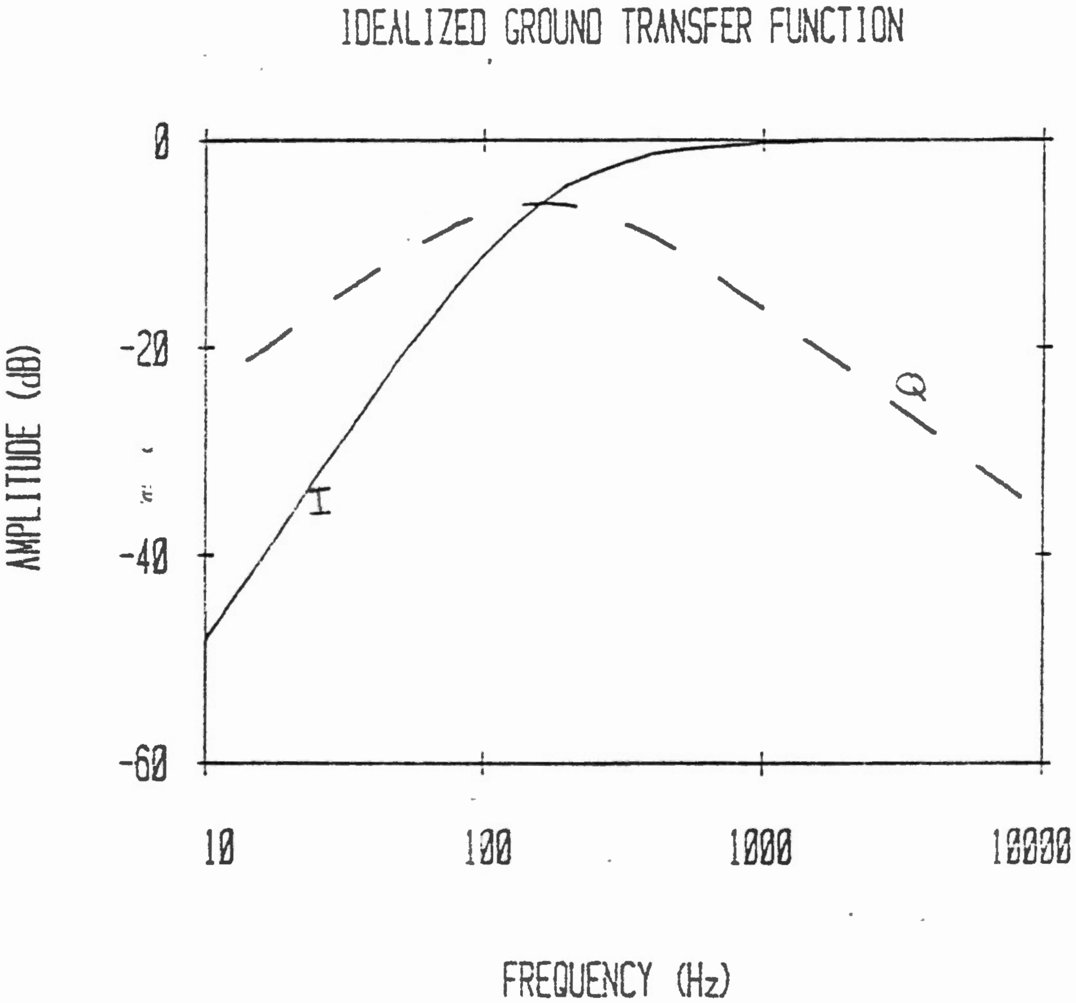
IDEALIZED GROUND TRANSFER FUNCTION

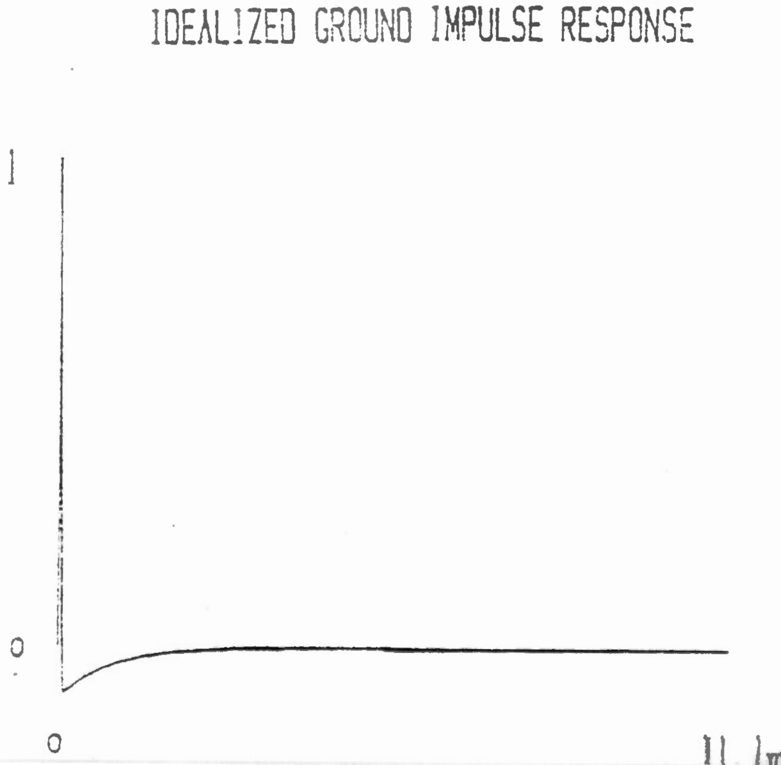
IDEALIZED GROUND IMPULSE RESPONSE

CONFIDENTIAL INFORMATION

FIG 2.2

COTRAN SYSTEM RESPONSES FOR IDEALIZED SQUARE WAVE

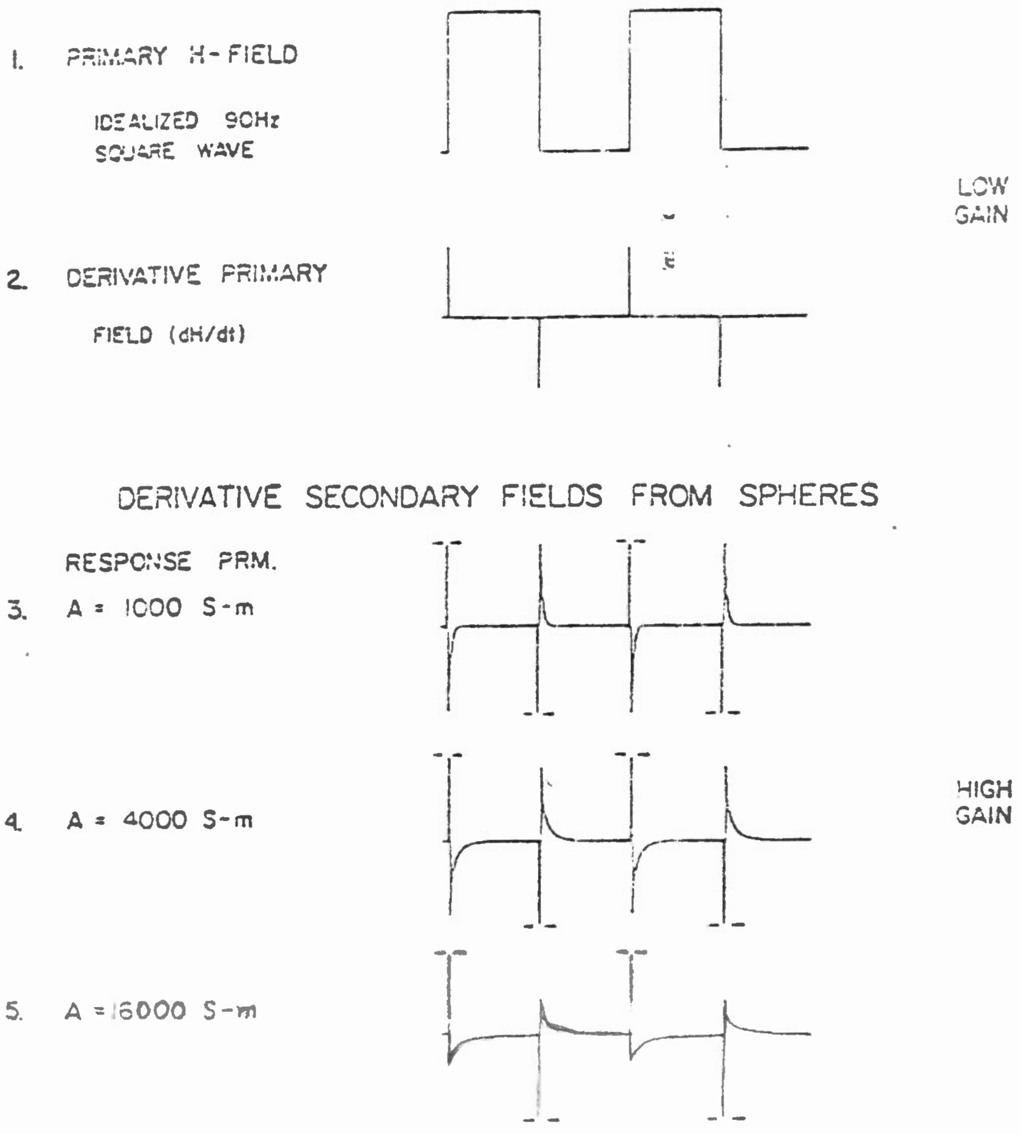

A = CONDUCTIVITY × RADIUS^2

CONFIDENTIAL INFOR[illegible]ATI
THIS DOCUMENT CONTAINS INF[illegible]MA
PROPRIETARY TO BARRINGER RESEA
LIMITED AND SHALL NOT BE REPRODU
OR TRANSFERRED TO OTHER DO[illegible]ME
OR DISCLOSED TO OTHERS, OR [illegible]ED
ANY PURPOSE OTHER THAN THAT
WHICH IT IS FURNISHED WITHOUT
PRIOR WRITTEN PERMIS[illegible]ON
BARRINGER RESEARCH LIMITE

FIG. 2.3

With the COTRAN system, the overall ground impulse response function or transfer function is the quantity which is measured. The measured data is of finite precision, finite bandwidth and contains noise. The COTRAN concept is to obtain the best estimate of the $G(\beta)$ in the above formulation keeping in mind the constraints of the measured data. The approach used is to match filter the data with a pre-defined set of basis functions. The received signal is decomposed as a superposition of the basis functions on a minimum energy or least squares criteria. The signal decomposition provides a direct estimate of the impulse response function or the transfer function of the ground.

In order to put the COTRAN concept into perspective, Fig. 2-3 shows the response of spheres of different conductivity for a square wave primary field. The derivative of the primary and secondary field are shown since these use the signals seen by a receiving coil. For the range of conductivity-radius squared products shown, the secondary response varies from appearing like the derivative of the primary field to looking very similar to the primary field. In all cases, there is a finite decay time for the secondary field. While ground responses vary in detail from the sphere response, the general nature of the response is the same. Fig. 2-4 shows the same sphere responses obtained using the band limited COTRAN square wave excitation.

The COTRAN matching procedure is based on the premise that

$$G(\beta) = \sum_{n=1}^{N} a_n Sn(\beta)$$

where the $S_{n(\beta)}$ are a set of causal basis functions a linear combination of which can approximate any ground response $G(\beta)$

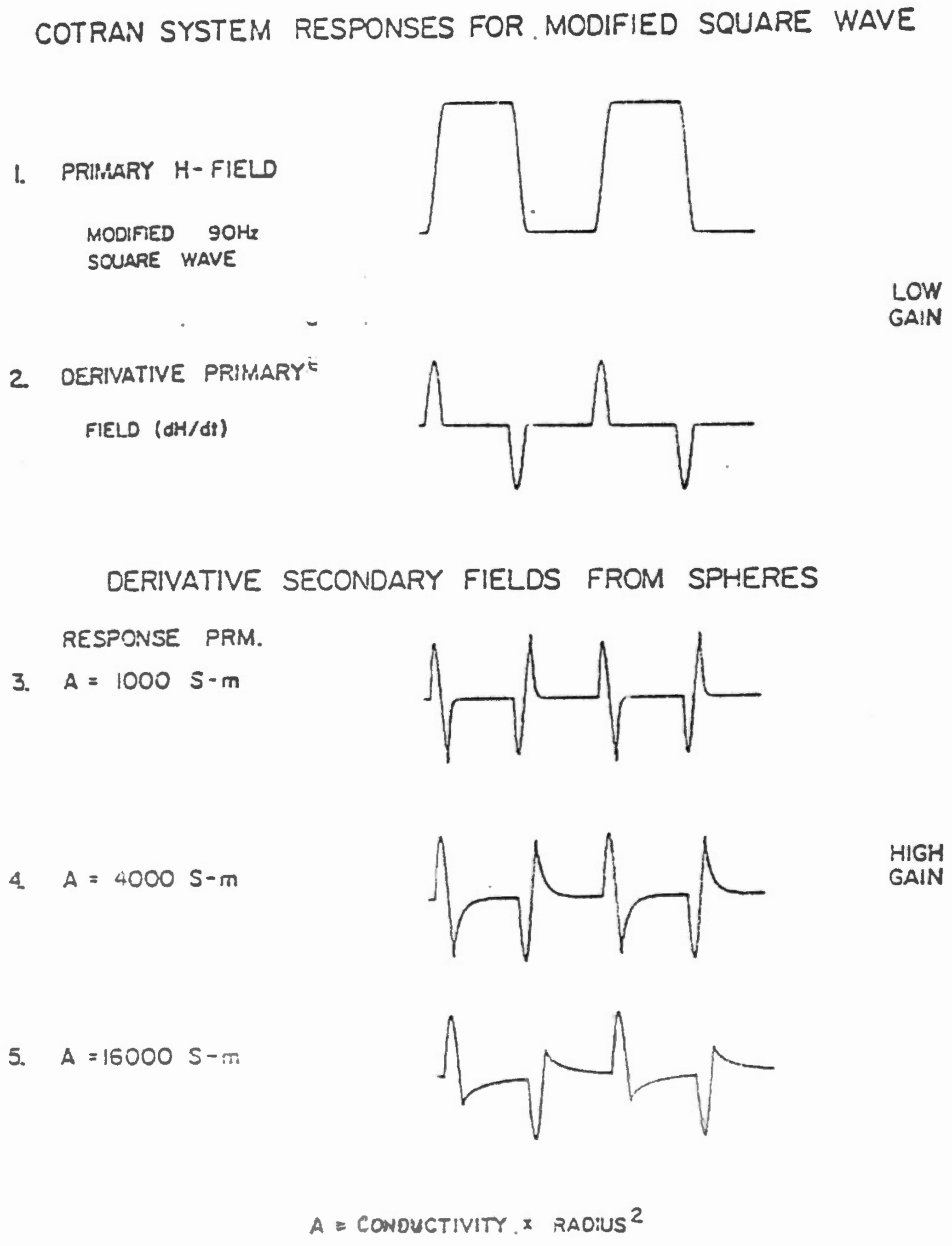
COTRAN SYSTEM RESPONSES FOR MODIFIED SQUARE WAVE
1. PRIMARY H-FIELD
MODIFIED 90Hz SQUARE WAVE
LOW GAIN
2. DERIVATIVE PRIMARY FIELD (dH/dt)
DERIVATIVE SECONDARY FIELDS FROM SPHERES
RESPONSE PRM.
3. A = 1000 S-m
4. A = 4000 S-m
HIGH GAIN
5. A = 16000 S-m
A = CONDUCTIVITY x RADIUS²

FIG. 2.4

to any required degree of accuracy. In theory, the number N is infinite. In practice with data of finite precision and finite noise levels, the number of matching functions is finite since the data can only be analysed to a finite level of accuracy.

On the assumption that P(t) is known, one postulates that

$$R(t) = a_o P(t) + \sum_{n=1}^{N} a_n \int_0^{\infty} S_n(\beta) P(t-\beta) d\beta + e(t)$$

where e(t) is the error induced by matching and the noise inherent in the data. The unknown coefficients a_i, i = o to N are estimated by minimizing the error e(t). For data from a finite time window width A which is usually one cycle of P(t) if P(t) is periodic, the error energy is defined as

$$E = \int_0^A e^2(t)\, dt$$

The optimal matching coefficients are then obtained by requiring

$$\frac{\partial E}{\partial a_i} = 0$$

The result is a set of linear equations in the unknown a_i which have to be solved.

Fig. 2-5 illustrates the decomposition of a sphere response using a set of pure exponential basis functions. The exponential response is the response which is obtained from a simple wire loop with resistance R and inductance L. The decay time or time of a constant eddy current in the loop is the L/R ratio. In Fig. 2-5, the top waveform is the response of a sphere to the band limited, 90 Hz COTRAN square wave. The

COTRAN SYSTEM - SYNTHESIS OF SECONDARY FIELD FROM SPHERE

1. SECONDARY FIELD FROM SPHERE

(σr^2 = 4000 S-m)

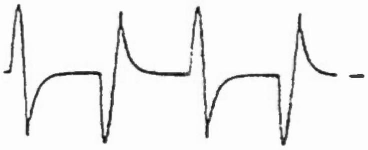

SYNTHESIS IN TERMS OF SECONDARY FIELDS FROM CONDUCTING LOOPS

	TIME CONSTANT		REL. AMP.
2.	τ = 30 μs	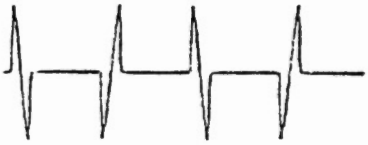	·083
3.	τ = 90 μs	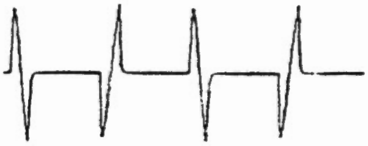	·061
4.	τ = 270 μs	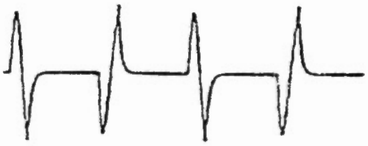	·529
5.	τ = 810 μs	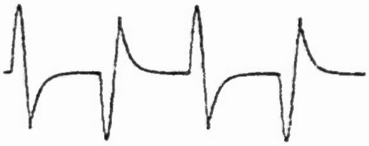	·308
6.	τ = 2430 μs		·017

FIG. 2.5

bottom set of waveforms is the set of COTRAN waveforms obtained by convolving the COTRAN waveform with exponential or loop responses with time constants of 30, 90, 270, 810 and 2430 microseconds. The amplitude of each component in the match is listed beside the waveform. In this case, the functions are

$$S_n(t) = \delta(t) - \frac{e^{-t/\tau_n}}{\tau_n} H(t)$$

where $\delta(t)$ is the Dirac delta function, $H(t)$ is the Heaviside step function, and τ_n is the time constant of the loop response. Further discussion of these basis functions is given in section 4 of this report.

When a data record has been processed, the optimal estimate of the ground over the entire frequency band of the system becomes available. Since the whole waveform is used in the process the overall character of the ground response is parameterized into a readily useable form. The power of the matching procedure is that it strongly rejects noise which is not causably related to the transmitter. In the frequency domain, coherency from one frequency to another is achieved by the imposition of causability on the observed response. The ground response can be displayed in both the time or frequency domain by synthesizing the ground response from a superposition of the known basis functions.

In order to carry out the COTRAN matching there are two prerequisites. The first is the availability of a wide band EM hardware unit which will collect the data with sufficient accuracy and reliability to allow the COTRAN procedure to be applied. The second requirement is a set of specific computer software which can handle the collected data in a routine and efficient manner. In general these two requirements are tightly interlinked. In the following two sections, the implementation of the COTRAN concept as a viable prototype hardware and data processing package is described.

3. COTRAN AEM SYSTEM DESCRIPTION

The COTRAN AEM system is a wide bandwidth, fixed-wing towed-bird system. Fig. 3-1 illustrates the system configuration. The system is mounted in a Super Canso operated by Geoterrex Ltd. A block diagram of the system is shown in Fig. 3-2. The following discussion gives a brief description of the system hardware and data acquisition procedure.

3.1 EM Hardware:

The transmitter loop is suspended from the nose, wing tips and tail of the aircraft. The loop has a cross sectional area of 260 m^2 and has six turns of wire. The transmitter electronics drive a square wave current with cosinusoidal switching shape at the polarity changes through the loop. The peak-to-peak current is 120 amps which produces a peak-to-peak vertical dipole moment of 186000 Am^2. The fundamental period of the transmitter current is selected to be 90 Hz. This fundamental frequency permits maximum rejection of 60 Hz interference in areas with cultural interference. The switching time for polarity transition is 1 millisecond. Fig. 3-3 illustrates the transmitter current or dipole moment and the voltage observed with a receiving coil as a function of time for one full transmitter cycle. Fig. 3-4 shows the amplitude spectrum of the receiving coil waveform. The voltage amplitude spectrum and waveform are particularly important since the eddy currents induced in the ground are energized by this signal which is proportional to the rate of change of magnetic flux density. Fig. 3-5 illustrates the direction of the primary magnetic field in space about the aircraft. This diagram is useful for understanding the coupling of the transmitted signal with discrete conductors below the aircraft.

COTRAN® AIRBORNE EM SYSTEM CONFIGURATION

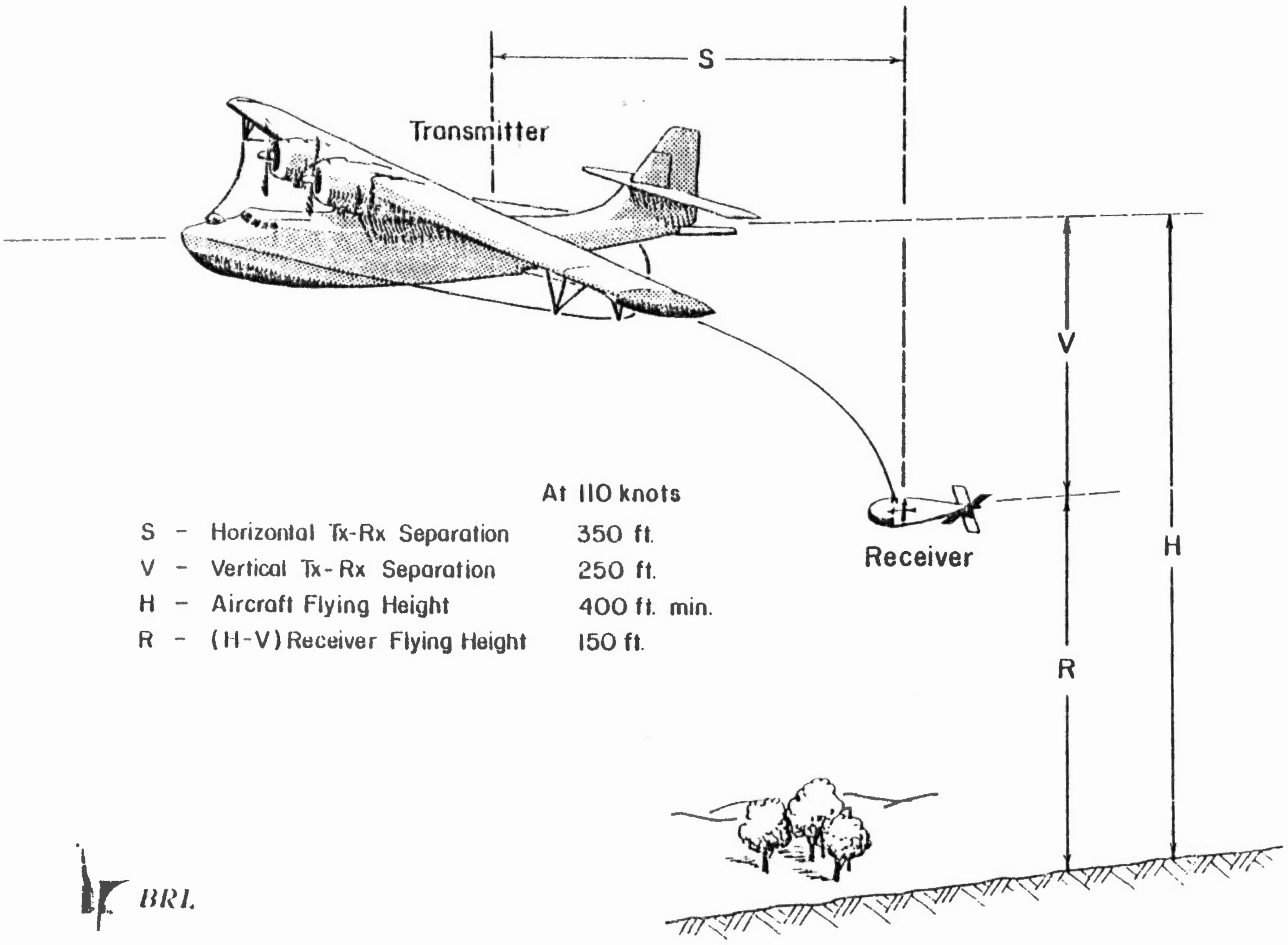

			At 110 knots
S	–	Horizontal Tx-Rx Separation	350 ft.
V	–	Vertical Tx-Rx Separation	250 ft.
H	–	Aircraft Flying Height	400 ft. min.
R	–	(H-V) Receiver Flying Height	150 ft.

BRL

FIG. 3.1

Hardware Block Diagram

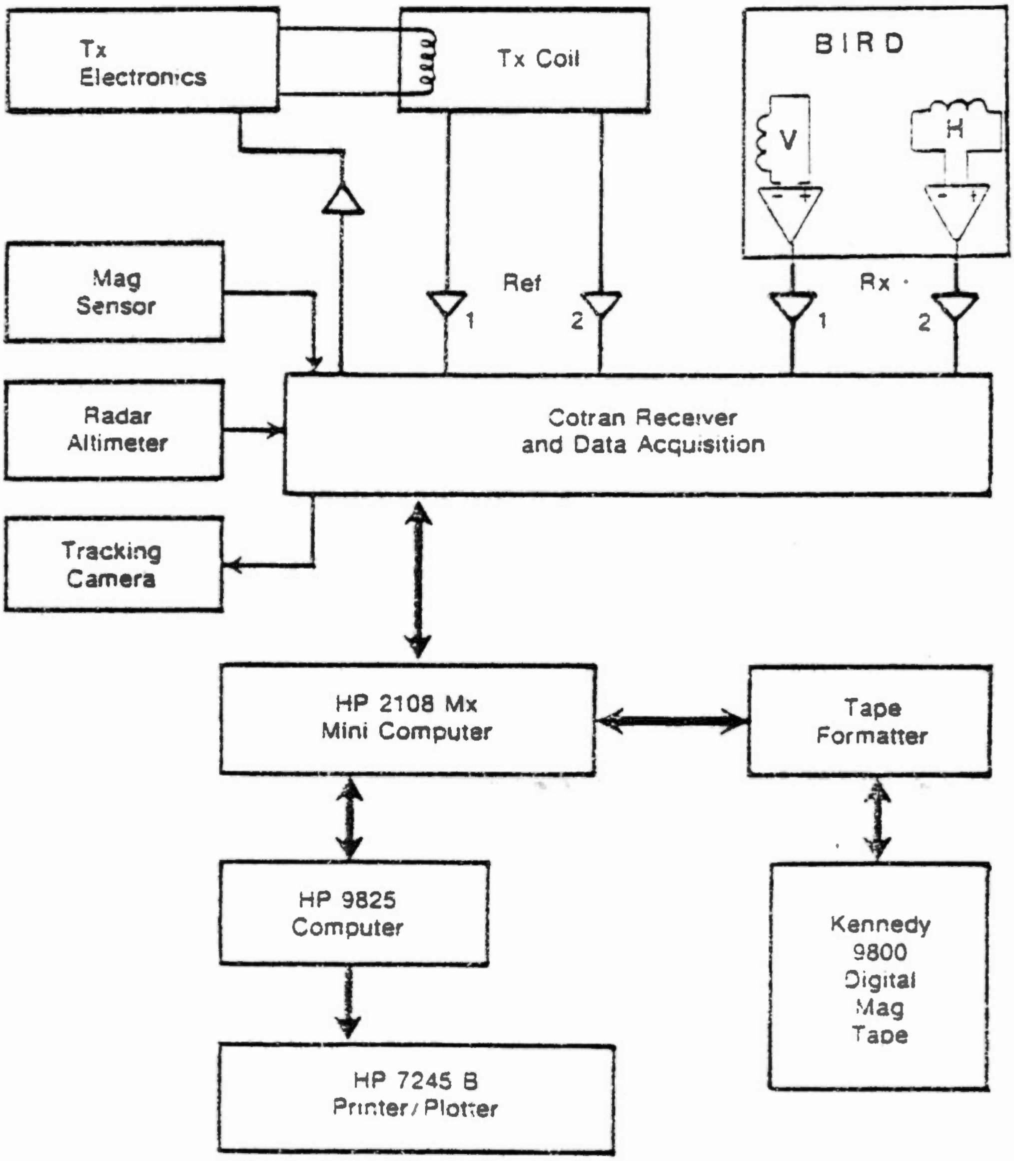

FIG. 3.2

COTRAN WAVEFORMS

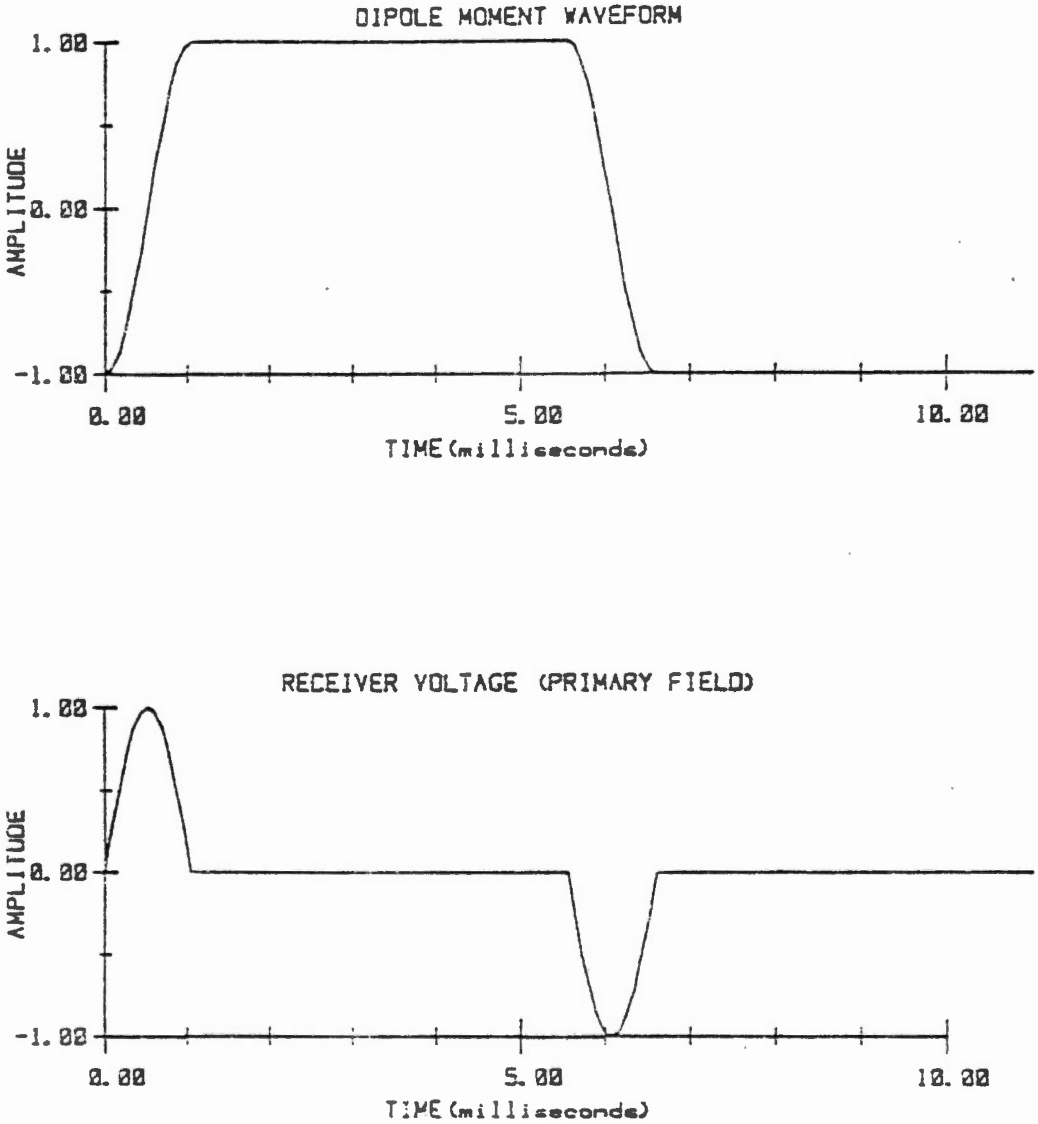

FIG. 3.3

AMPLITUDE SPECTRUM OF RECEIVER WAVEFORM

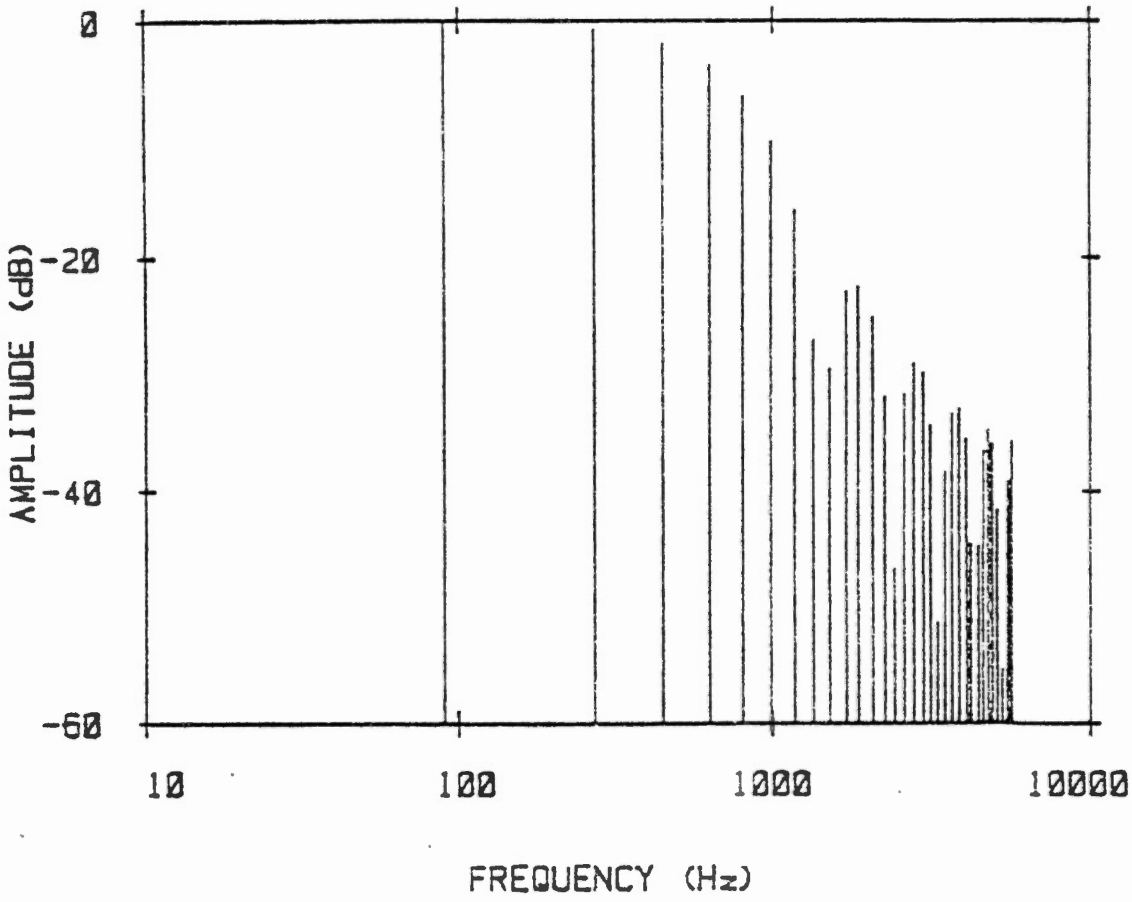

PRIMARY FIELD DIRECTION

VERTICAL MAGNETIC DIPOLE AT 170 m HEIGHT

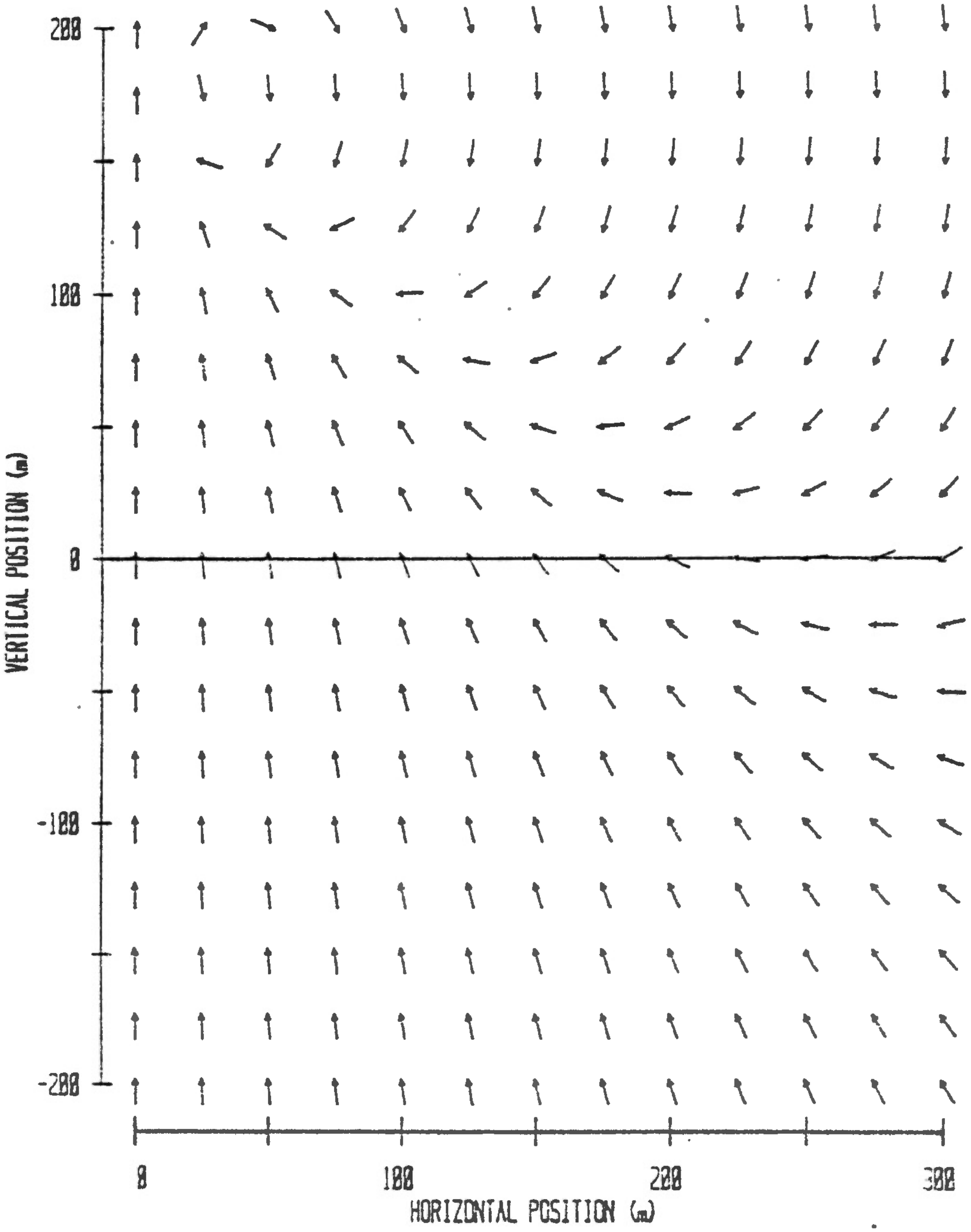

FIG. 3.5

The response of the ground is sensed by two orthogonal receiving coils mounted in a towed-bird. The coils form a rigid unit which is gimbal mounted in the bird. One coil has its axis aligned in the flight direction while the other coil has its axis aligned in the vertical direction. The bird and coil suspension system have been designed to minimize coil motion and vibration. The high fidelity broadband coil system feeds the received voltage to battery powered preamps which are also mounted in the bird. The amplified signal is then fed to the COTRAN receiver in the aircraft via electrical conductors in the tow cable.

The COTRAN receiver consists of 4 identical receiving channels. Each channel has an identical set of RF, high pass, and low pass (anti-aliasing) filters. The two channels assigned to the signals received at the bird also have a feedback, 60 Hz rejection filter. The four channels are then fed to a sample-hold and A/D conversion unit which samples the four channels at a rate of 128 times per transmitter cycle. With a transmitter fundamental frequency of 90 Hz, this corresponds to a sampling interval rate of 86.7 microseconds and a Nyquist frequency of 5760 Hz.

Two of the receiver channels are assigned to the signals from the two receiving coils in the bird. The other two channels are assigned to monitoring the transmitter waveform. One channel uses a toroidal ferrite current transducer mounted around the transmitter feed cable to monitor the actual current in the transmitter loop. The other channel measures the rate of change of the transmitter dipole moment by sensing the voltage induced in a single turn of wire which is mounted in coincidence with the transmitting loop.

3.2 Auxiliary Hardware:

In addition to the EM hardware, the COTRAN system has a Barringer proton precession magnetometer, a 35 mm strip camera for flight path recovery, a radar altimeter, a 60 Hz monitor, a spherics killer unit, a low speed real-time peripheral (RTP) interface unit and an aircraft orientation sensor.

The magnetometer sensor is located in a fibreglass tail stinger. The signal processing and magnetometer control unit is mounted in the COTRAN receiver package. The magnetometer will only function when the COTRAN transmitter is turned off. As a result, the magnetometer and COTRAN transmitter are synchronized to operate in a time sharing arrangement. More detail on this time sharing arrangement will be given later in the section on data acquistion procedure.

The 35 mm strip camera is a standard flight path recovery camera. The automatic fiducial number generated by the computer system is fed to the camera via the RTP unit. Every tenth fid number is superimposed on the film strip.

The altimeter is a Sperry radar altimeter (FM-CW) which forms part of the aircraft instrumentation package. The altimeter output is an analog signal which goes to the cockpit instrumentation panel and is fed in parallel to the RTP interface unit where it is digitized and passed to the HP2108.

The 60 Hz monitor unit is designed to measure the ambient 60 Hz powerline interference in the vicinity of the bird. The signal received from the vertical axis coil in the bird is tapped and passed through a tuned 60 Hz filter. The signal is then rectified and integrated. The slowly varying output of the 60 Hz monitor is then passed to the RTP unit where it is digitized and made available to the HP2108 computer.

The spherics killer unit is a module designed to eliminate cycles of EM data which are contaminated by large local spherics. This unit cannot remove the ambient background spherics noise. The unit ping-pong buffers the digitized output of the COTRAN receiver. The full 128 point waveform for all four channels is fed into one buffer. At the same time, an analog circuit fed by either the horizontal axis receiver coil signal or a small vertical whip antenna mounted on the aircraft senses the presence of spheric transients above a variable threshold during the EM cycle. If a spheric is detected, the current EM data buffer is dropped. If no spheric is detected the waveforms are passed on to the HP2108. While the decision to drop the previous cycle of data is being made or while the previous cycle data is being passed to the HP2108, the EM data from the current cycle is stored in the other buffer of the spherics killer. In operation, the HP2108 expects a fixed number of cycles of data from the EM system. If a cycle is dropped, the EM system runs for an extra cycle to make up for the dropped data. In bad spherics conditions, or with a very low threshold setting, many or all cycles may be dropped. To eliminate hanging the whole system, the spherics killer counts the number of cycles dropped. When the count reaches 10 cycles, the spherics killer deactivates itself and passes data continually to the HP2108 until the required number of cycles of data have been obtained. The spherics killer can be switched in and out of the system as desired.

The RTP interface unit handles all low speed analog and digital I/O to and from the HP2108. In the current configuration, the RTP digitizes 5 analog signals with 12 bit resolution. In addition, the RTP passes two 16 bit digital inputs to the HP2108 and passes the BCD encoded fid number to the flight path recovery camera.

The aircraft orientation monitor is a three component fluxgate magnetometer which provides a 3 channel analog output of the aircraft orientation using the ambient Earth field in the flight area. These three analog signals are passed to the RTP unit which digitizes the signals and passes them on to the HP2108.

3.3 Computer Control and Data Acquisition:

The overall operation of the system is controlled by the HP2108 and HP9825 computer system. The HP9825 is the master computer and the HP2108 acts as a slave and controls data acquisition. The operator interacts with the system via the HP9825 keyboard and LED display. Tasks for the two systems are clearly divided. The HP2108 acquires the EM data and the low speed peripheral data. This data is put into a standard format and written to tape and to the HP9825 by the HP2108 during data acquisition. During data replay, the HP2108 reads the data back from tape and passes it to the HP9825.

The HP9825 controls the mode of operation of the HP2108. In addition, the HP9825 carries out the COTRAN processing of the EM data and lists and/or plots profiles of the EM data and the low speed data on the HP7245B printer/plotter. The real-time listing or plots permit monitoring of overall system performance during flight.

The pertinent aspect of the computer system is the manner in which it controls and acquires data at a given fid. The procedure at each fid is as follows. First the computer automatically increments the fid counter on each data acquisition cycle. The computer then turns the COTRAN transmitter on and the COTRAN receiver starts acquiring data after the transmitter has been turned on for 8 full cycles. This delay permits stabilization of the switch-on transients.

The HP2108 accepts the 4 sampled EM waveforms from the COTRAN receiver and stacks or coadds a software defined number of full cycles of EM data. The number of cycles coadded is an integer value between 0 and 128. Normally, the number of cycles is chosen to be a multiple of 3 in order that a complete number of 60 Hz interference noise is accomodated. For most work, the number of cycles stacked is 126.

Once the HP2108 has acquired the desired number of cycles of EM data, the COTRAN transmitter is turned off. The HP2108 next reads in the data from the slow speed peripherals which includes the magnetometer data which is acquired while the transmitter is off. All the data is stored in a buffer in a pre-defined format and output to the HP9825 and the tape drive. This information constitutes one fid of data. The time required to acquire the data is

$$T = 400 + 11.11N \text{ milliseconds}$$

where N is the number of EM cycles stacked and 11.11 is the period of the COTRAN transmitter waveform assuming a 90 Hz fundamental frequency. The constant 400 milliseconds is the dead time required for housekeeping in the computers, reading of the mag data and settling of the EM system at switch-on. The time required for data acquisition is akin to the time constant of conventional analog EM systems.

In data acquisition mode, the HP2108 continually repeats the sequence of events described above. The acquisition is terminated by a command from the HP9825 when the operator indicates the end of a survey line. In addition to controlling data acquisition, the computer system also maintins a flight directory and a log of the names of flight lines, the initial and final fid number for each line and a set of comments for each line. This information is written onto the beginning of each COTRAN data tape. The format of a COTRAN data tape is summarized in Appendix A.

3.4 General Summary:

The preceding discussion gives a general overview of the hardware and data acquisition aspects of the COTRAN system. An overall summary of the COTRAN hardware is given in Table 1.

TABLE 3-1

COTRAN SYSTEM PARAMETERS

General

Aircraft	Super Canso
System Type	Towed Bird

Transmitter

Orientation	Vertical Axis Dipole
Peak-to-Peak Moment	186000 Am2
Current Waveform	Square wave with cosinusoidal switching
Fundamental Frequency	90 Hz
Fundamental Period	11.11 ms
Switching Time	1 ms

Towed Bird

Receiving Coils	1 vertical axis 1 horizontal axis in flight direction
Coil Effective Area	30 m2
Tow Cable Length	160 m
Bird Position (nominal)	110 m behind aircraft 90 m below aircraft
Peak-to-Peak Primary at Bird (nominal)	4.9 nT

4 Channel
Receiving Electronics (Analog)

Filters

Low pass AA	3.5 kHz active
High pass	7 Hz active
RF	passive

4 Channel
Receiving Electronics (Digital)

A/D	12 bit
Sampling Interval	86.8 us
Sampling Rate	11520 Hz
Nyquist Frequency	5760 Hz
No. of Points/Cycle	128
Spherics Killer	Variable Threshold

Channel Assignment

Channel 1	Transmitter voltage reference
Channel 2	Transmitter current reference
Channel 3	Horizontal axis receiver
Channel 4	Vertical axis receiver

Airborne Computing

Computers	HP2108 mini computer HP9825 desk-top computer
Data Display	HP7245B thermal print/plot
Data Recording	9-track 800 bpi 7" tape

Auxiliary Equipment

Magnetometer	Barringer Proton precession
Heading Indicator	3 component fluxgate
Altimeter	Sperry Radar Altimeter
Flight Path Camera	Geocam 35 mm strip camera

System Cycle Time

T = 400 + 11.11 N milliseconds

N = number of transmit cycles stacked

4. COTRAN DATA PROCESSING

4.1 FORMULATION OF THE LINEAR MATCHING PROCEDURE

The COTRAN EM data consists of 4 waveforms each of 128 points when it arrives at the data reduction stage. Each waveform represents the average of a number of repetitions of the transmitter cycle. In this section, the general mathematical formulation for the matching procedure is developed for the specific COTRAN data format.

First, the waveforms are noted by

$$p_i \qquad i = 1 \text{ to } 128$$
$$h_i \qquad i = 1 \text{ to } 128$$

where p_i denotes the transmitted primary waveform as a function of time, h_i denotes the waveform from the horizontal or vertical axis receiving coil. Both h_i and p_i are considered as one cycle of a periodic time series with 128 point period. Since the waveforms are sampled at equally spaced time intervals Δt, analysis of the signal can be carried out in either the time domain or the frequency domain with the aid of the Fast Fourier Transform (FFT). Depending upon the type of data manipulation to be carried out, one domain may prove more efficient than the other for data processing. The result of the processing is independent of the domain chosen for operation. In the following, the basic processing for both domains is outlined.

(a) Time Domain Formulation:

The time domain matching requires definition and computation of the set of basis impulse response functions which are to be used approximate the ground response. The digitized impulse response basis functions are defined as

$$g_i^j \qquad i = 1 \text{ to } M_j \qquad j = 1 \text{ to } N$$

where g_i^j is the i th point of the j th impulse response basis function which has a length of M_j points. Details of the selection of the basis functions are given in the next section of this report.

The next step is to carry out the periodic or circular convolution of the impulse response basis functions with the excitation or primary field waveform p_i. The waveforms obtained are defined as

$$f_i^j \qquad i = 1 \text{ to } 128 \qquad j = 1 \text{ to } N$$

where

$$f_i^j = \sum_{q=1}^{M_j} g_q^j \, p_{(i-q+1) \bmod 128}$$

where

$$\begin{aligned} A \bmod B &= A - B \text{ integer } (A/B) && A \geqslant 0 \\ &= A + B - B \text{ integer } (A/B) && A < 0 \end{aligned}$$

The set of N waveforms f_i^j represent the basis for matching the ground response waveforms.

The observed waveform h_i is now postulated to have the form

$$h_i = a_0 p_i + \sum_{j=1}^{N} a_j f_i^j + e_i$$

where a_j are a set of unknown amplitude coefficients and e_i is the matching and random noise error combined at time i. For convenience in the following derivation it is best to define

$$f_i^0 = p_i$$

such that

$$h_i = \sum_{j=0}^{N} a_j f_i^j + e_i$$

The objective now is to ascertain the N + 1 unknown coefficients a_j, j = 0 to N.

There are numerous criteria which may be applied to estimate the a_j. The approach found most useful and reliable for handling COTRAN data has been the minimization of the error energy which is a least squares technique. The total error energy E is defined as

$$E = \sum_{i=1}^{128} e_i^2$$

In some instances, a weighted or bias error energy estimator is useful, namely

$$E = \sum_{i=1}^{128} w_i e_i^2$$

where w_i is a positive definite weighting function (i.e., $w_i > 0$) such that

$$\sum_{i=1}^{128} w_i = 1$$

The solution for the a_j's is then selected as the set of a_j which minimize E. The use of a weighting function permits emphasis or de-emphasis of particular parts of the waveform in time. In practice, little is gained by non-uniform weighting unless a particular part of the time series is noisy and should be de-emphasized.

The set of a_j which minimize E are defined by the set of normal equations

$$\frac{\partial E}{\partial a_j} = 0$$

The resulting set of linear equations take the form

$$C_{ij}\, a_j = D_i$$

where

$$C_{ij} = \sum_{q=1}^{128} w_q\, f_q^i\, f_q^j$$

$$D_i = \sum_{q=1}^{128} w_q\, h_q\, f_q^i$$

The C_{ij} are the weighted cross covariance of zero lag between the basis waveforms. The D_i are the weighted cross covariance of zero lag between the basis functions and the received waveform. Inversion of the N+1 x N+1 correlation matrix yields the solution of the a_j with

$$a_j = C_{ji}^{-1} D_i$$

with the corresponding error

$$E = \sum_{q=1}^{128} W_q h_q^2 - \sum_{j=0}^{N} a_j D_j$$

This constitutes the formal solution of the linear matching problem. The practical limitations of implementing the procedure are discussed later in this section of the report.

(b) Frequency Domain Formulation:

The frequency domain formulation follows the same procedure as the time domain matching formulation. First the set of transfer functions corresponding to the set of basis impulse response functions are defined as

$$G_i^j \quad i = 1 \text{ to } 65 \qquad j = 1 \text{ to } N$$

where the G are complex numbers representing the in-phase and quadrature components of the transfer functions at the harmonic frequencies $\Delta f(i-1)$

where

$$\Delta f = \frac{1}{128 \Delta t}$$

The next step is to FFT the primary reference waveform and the observed waveforms with

$$P_j = \sum_{k=1}^{128} p_k \, e^{i2\pi\left(\frac{jk}{128}\right)}$$

$$H_j = \sum_{k=1}^{128} h_k \, e^{i2\pi\left(\frac{jk}{128}\right)}$$

Of the 128 values of the spectra P_j and H_j only the first 65 are unique. The fact that p_k and h_k are real time series requires

$$P_j = P^*_{130-j} \qquad j = 66 \text{ to } 128$$
$$H_j = H^*_{130-j}$$

where * denotes the complex conjugate operation.

The FFT operation translates the circular convolution operation into a multiplicative operation. The basis functions for matching are defined as

$$F_i^j = G_i^j \; P_i \qquad i = 1 \text{ to } 65$$

Each spectral component of the excitation signal is multiplied by the transfer basis function G_i^j to obtain the set of functions for matching the ground response.

In the matching process, the observed signal is postulated to be of the form

$$H_i = a_0 P_i + \sum_{j=1}^{N} a_j F_i^j + e_i$$

where e_i is the combined error at frequency $\Delta f(i-1)$ generated by noise in the data and inadequacy of the matching functions. As in the time domain, it is convenient to denote

$$F_i^0 = P_i$$

such that

$$H_i = \sum_{j=0}^{N} a_j F_i^j + e_i$$

The a_j coefficients are determined by minimizing the error energy. Utilizing the weighted error energy estimate, the error energy is

$$E = \sum_{i=1}^{65} w_i |e_i|^2 = \sum_{i=1}^{65} w_i e_i e_i^*$$

Minimization of E with respect to the unknown coefficients a_j yields the set of normal equations

$$\frac{\partial E}{\partial a_j} = 0$$

which have the form

$$C_{qj} a_j = D_q$$

where

$$C_{q,j} = \sum_{i=1}^{65} w_i \left(F_i^q F_i^{j*} + F_i^{q*} F_i^j \right)$$

$$D_q = \sum_{i=1}^{65} w_i \left(F_i^q H_i^* + F_i^{q*} H_i \right)$$

The error energy at the solution point has the form

$$E = \sum_{i=1}^{65} w_i H_i H_i^* - \frac{1}{2} \sum_{j=0}^{N} a_j D_j$$

where the solution vector of the a_j is

$$a_j = C_{jq}^{-1} D_q$$

The expression constitutes the formal solution in the frequency domain. The only difference between the two approaches is that the weighting function in the error analysis is multiplicative. As a result, the two solutions are identical only if w_i = constant.

4.2 SELECTION OF BASIS MATCHING FUNCTIONS

A key part of the matching process is the selection of the impulse response basis functions. There is a wide range of possibilities to choose from with the only constraint being that of causality. Ideally, the basis functions should resemble the ground responses normally observed to a reasonable degree. In addition, the basis functions should be easy to parameterize and easy to synthesize on a digital computer.

Experience with INPUT data and other transient systems suggests that transient responses frequently are nearly pure exponential decays. Furthermore, the limiting long-time response of discrete, finite dimension conductors is known to be purely exponential from a theoretical basis. While the exponential response is not valid for bodies of infinite extent, over a finite time window, it is often very difficult to discern the differences between a superposition of exponential decays and the power-law fall off which is the true behaviour. From these considerations plus the practical advantages of simple parameterization and ease of computation, the basis functions for the bulk COTRAN matching were selected to be of exponential form.

The specific form of the exponential basis function model is derived from the response of a simple wire loop. From Appendix C, the transfer function of a wire loop with inductance L and resistance R has the form

$$H(\omega) = \frac{i\omega\tau}{1 + i\omega\tau}$$

where

$$\tau = L/R$$

is the time constant of the loop and ω is angular frequency. The corresponding impulse response function is

$$h(t) = \delta(t) - \frac{e^{-t/\tau}}{\tau} \mathcal{H}(t)$$

where $\delta(t)$ is the Dirac delta function and $\mathcal{H}(t)$ is the Heaviside step function.

The simple exponential or loop response model is a good choice for the basis functions because the eddy currents induced in distributed conductors in the ground frequently approximate the behaviour of current induced to flow in a wire loop. Therefore, there is a strong physical basis for understanding data decomposed in this manner. In fact, the time constant of a distributed eddy current flow in a conductor has the form

$$\tau = \mu \sigma L_1 L_2$$

where u is the magnetic permeability and σ is the conductivity of the conductor. L_1 and L_2 are two spatial dimensions which characterize the cross sectional area of the distributed current flow.

Upon acceptance that the loop model will provide a sound basis function, the next step to address is how to incorporate the model into the COTRAN matching procedure. A number of alternatives have been examined. One possibility is to attempt to model the ground response with a function of the above form with an unknown amplitude and time constant which best approximates the data. Unfortunately, this approach leads to a non-linear problem which requires an iterative solution. Furthermore, observed ground responses seldom behave as simple exponential responses and are best characterized as a superposition of several exponential decay terms. While this approach has been studied in some detail, it was ruled out as a viable method for bulk data reduction. This decision, however, should not preclude future investigation and possible implementation of such a scheme.

Since a superposition of exponential decays appears to be most appropriate for approximating ground responses, a model which yields a linear matching problem and incorporates superposition was selected, namely,

$$h(t) = \int_0^\infty A(\tau)\left(\delta(t) - \frac{e^{-t/\tau}}{\tau} H(t)\right) d\tau$$

Here the problem of estimating τ is replaced by the determination of an amplitude spectrum for τ . This particular model possesses all the desired characteristics but has an infinite number of degrees of freedom. In order to employ this model, practical constraints must be imposed upon the amplitude spectrum $A(\tau)$.

The first constraint which must be addressed is the finite bandwidth of the EM system which is used to make the measurements of the ground response. This constraint requires that

$$A(\tau) = 0 \qquad \tau > \tau_{max} \quad \text{and} \quad \tau < \tau_{min}$$

The system will only provide data which can resolve $A(\tau)$ over a finite range of time constants, namely, $\tau_{min} \leq \tau \leq \tau_{max}$. The appropriate form of h(t) is

$$h(t) = A_0 \delta'(t) + A_1 \delta(t) + \int_{\tau_{min}}^{\tau_{max}} A(\tau) \left[\delta(t) - \frac{e^{-t/\tau}}{\tau} H(t) \right] d\tau$$

The A_o term accounts for all responses with time constants less than τ min while the A_1 term accounts for all responses with time constants greater than τ max. The A_o term just yields the derivative of the primary excitation or all quadrature response. Such a response is observed when an EM system operates at the resistive limit of a target. The A_1 term yields a replica of the primary excitation field or all in-phase response. This response is observed with an EM system which operates at the inductive limit of a target.

The second constraint which must be addressed is the finite accuracy of the data. The finite digital resolution and noise levels of the data limit the degree to which $A(\tau)$ can be resolved from the data. The practical approach to this limitation is to place an a priori constraint on the degrees of freedom permitted for $A(\tau)$ in the range τ min $\leq \tau \leq \tau$ max. The simplest and most practical form for $A(\tau)$ is

$$A(\tau) = \sum_{p=1}^{N} a_p \, \delta(\tau - \tau_p)$$

In other words, $A(\tau)$ is digitized at a discrete set of values. Other more complex forms were considered for $A(\tau)$, such as piece wise linear and power series expansions. The added complexity of such formulations yielded little benefit and was dropped from consideration for routine processing. The problem left to be addressed with the above model is the selection of the τ_p values. Extensive examination of the stability of the COTRAN matching formulation resulted in a general rule that the τ_p have the form

$$\tau_p = 3^{p-1} \tau_{min} \qquad p = 1 \text{ to } N$$

In other words, real data was incapable of resolving responses where time constants were closer than a factor of 3 apart. Obviously the above result is empirical in nature and is very dependent on the system characteristics and noise levels.

The final model for h(t) is a discrete set of exponential or loop response models. The model is regrouped in the form

$$h(t) = \sum_{j=1}^{N} a_j \left(\delta(t) - \frac{e^{-t/\tau_j}}{\tau_j} \mathcal{H}(t) \right)$$

where

$$\tau_1 = \tau_{min} / 3$$

$$\tau_j = 3^j \tau_1$$

and

$$N = \text{integer} \left(\log_3 \left(\frac{\tau_{max}}{\tau_{min}} \right) \right)$$

The very short time constant responses characterized by the A_o term discussed previously are lumped into the τ_1 term which has a time constant which is 1/3 of the minimum resolvable time constant. This is just a convenient method of incorporating the short time constant contribution into the postulated model. Energy in this component should not be construed as truly corresponding to a time constant τ_1 but rather as the lumped effect of all ground responses with $\tau < \tau$ min.

The very long time constant responses which were characterized by the A_1 term are not resolvable from primary field variations. As such, this term is dropped from the ground response model and picked up in the primary field estimation term.

To conclude this section, the basis functions developed here are placed in a format compatible with the formal matching scheme outlined in section 4.1. In section 4.1, the digitized time domain impulse response functions are denoted as g_n^j and the frequency domain transfer functions are G_n^j . Assuming a periodic excitation sampled at a rate of 128 points per cycle which results in a sampling interval Δt , the form of the g_n^j and the G_n^j is as follows.

Time Domain Digitized Basis Functions:

$$g_1^j = e^{-\Delta t/2\tau_j}$$

$$g_n^j = -e^{-(2n-3)\Delta t/2\tau_j}\left(1 - e^{-\Delta t/\tau_j}\right) \qquad n = 2 \text{ to } M_j$$

where M_j is chosen such that $\left| g_{M_j}^j / g_1^j \right| < 10^{-4}$

Frequency Domain Basis Functions:

$$G_n^j = \frac{i\,(n-1)\,\pi\,\tau_j\,/64\Delta t}{1 \;+ i\,(n-1)\pi\;\tau_j\,/64\Delta t}$$

For the current COTRAN system configuration, the values of τ min and N are

min = 90μs
N = 5

which yields a set of τ values of 30, 90, 270, 810 and 2430 microseconds.

4.3 RECEIVING COIL MOTION EFFECTS

The EM response of the ground is measured with a coil which senses the changes of magnetic flux which passes through the coil. For any airborne system, a receiving coil is in constant motion with magnitude of the motion being dependent on the system configuration. In order to account for motion effects in a rational manner, this section reviews the basics of induction of voltage in a coil. The open-circuit voltage of a small coil with effective area A_e and axis aligned in direction $\hat{n}$ is

$$V(t) = \frac{d}{dt}\,(A_e\overline{B}.\hat{n})$$

where $\overline{B}$ is the magnetic field at the receiving coil. $\overline{B}$ is assumed to be uniform over the spatial dimensions of the coil. Expanding V(t) in detail yields

$$V(t) = A_e \left(\hat{n} \cdot \frac{\partial \bar{B}}{\partial t} + (\bar{u} \cdot \bar{\nabla}) \bar{B} \cdot \hat{n} + \bar{B} \cdot \frac{\partial \hat{n}}{\partial t} \right)$$

where the first term represents the voltage induced by temporal variation in B alone. Ideally, this is the only signal which is to be detected. The second term represents the voltage induced in the coil by translation of the coil with velocity $\bar{U}$ through a magnetic field gradient. The third term represents the voltage induced in the coil by rotation of the axis of the receiving coil with time. The latter two terms represent motion noise in an EM system.

One form of noise is Earth's field noise which is generated by the fact that the coil is moving in the Earth's static magnetic field $\bar{B}_e$. Earth's field noise is defined as

$$V_e(t) = A_e \left(\bar{u} \cdot \bar{\nabla} \bar{B} \cdot \hat{n} + \bar{B}_e \cdot \frac{\partial \hat{n}}{\partial t} \right)$$

To a very good approximation, the second term is the dominant component of V_e.

The other form of motion noise is the movement of the coil in the primary EM field, B_p. The primary field motion noise has the form

$$V_p(t) = A_e \left(\bar{u} \cdot \bar{\nabla} \bar{B}_p \cdot \hat{n} + \bar{B}_p \cdot \frac{\partial \hat{n}}{\partial t} \right)$$

The movement of the coil in the secondary field from the ground, $\bar{B}_s$ also generates motion noise but $|\bar{B}_s|$ is usually much less than $|\bar{B}_p|$ and is a minor problem.

With careful coil suspension system design, the motion terms $(\bar{u} \cdot \bar{\nabla})$ and $\partial \hat{n} / \partial t$ are very slowly varying functions of time compared with the EM signal. As a result, V_e is a very low frequency signal and can be filtered out of the received signal to a very large degree. This is not the case for V_p even though the motion effects are slow. V_p also reflects the high frequency content of the primary field.

To a very good approximation, the received voltage from the coil becomes

$$V(t) = V_s(t) + V_p(t)$$

where

$$V_s(t) = A_e \hat{r} \cdot \frac{\partial \bar{B}}{\partial t} = A_e \hat{n} \cdot \frac{\partial}{\partial t} (\bar{B}_p + \bar{B}_s)$$

is the desired signal. From the COTRAN data processing point of view, the received signal can be expressed as

$$V(t) = A_0(t) P(t) + A_1(t) Q(t) + \int_0^\infty h(\beta) P(t-\beta) d\beta$$

where P(t) is the primary field waveform, h(t) is the impulse response of the ground and Q(t) is defined as

$$Q(t) = \int_{-\infty}^{t} P(\gamma) d\gamma$$

which is the waveshape of the primary magnetic field. The coefficients $A_o(t)$ and $A_1(t)$ are slowly varying amplitude modulation factors which reflect the $(\bar{u} \cdot \bar{\nabla})$ and $\partial \hat{n} / \partial t$ terms of V_p and V_s.

In order to accomodate these effects in the COTRAN processing, one can use a Taylor series expansion of A_o and A_1 to generate additional waveshapes to be matched.

For periodic excitation with stacking or coadding as part of the data acquisition, one can treat the signals on a cycle-by-cycle basis. Over one period of the data,

$$A_o(t) \simeq c_0 + c_1 t + c_2 t^2 + \ldots$$
$$A_1(t) \simeq d_0 + d_1 t + d_2 t^2 + \ldots$$

Using this approximation which is a valid assumption with good system design, the matching problem becomes the following

$$V(t) = a_0 P(t) + \sum_{n=1}^{N} a_n \int_0^{\infty} g_n(\beta)\, P(t-\beta)\, d\beta$$
$$+ a_{N+1} X(t) + a_{N+2} Q(t) + a_{N+3} Y(t)$$

where

$X(t) = t\ P(t)$
$Y(t) = t\ Q(t)$

Higher order terms of the series expansion could be retained but such terms will have negligible value with good system design. In order to accomodate bird motion effects, the standard matching procedure discussed previously is carried out but an additional 3 waveforms are added to the basic waveshape set.

Considerable testing of this approach has been carried out on selected portions of COTRAN data with some success.

Unfortunately, data quality is not in general limited by motion effects and only marginal improvement is observed when the motion removal procedure is applied to bulk data reduction. In general, the bird motion noise is not the limiting noise in the data. As system performance is improved, the need for removal of motion effects will become more important.

4.4 PRACTICAL IMPLEMENTATION OF MATCHING PROCEDURE TO ACCOMODATE LIMITATIONS OF DATA AND HARDWARE

The previous discussions in this section provide the general basis for the COTRAN matching operations. In practice, the general theoretical formulation has to be tempered by the true realities of the data quality. This section addresses the compromises which have to be made to make theory and reality mesh to give useable results. There are two problems to be addressed when working with real data. First and foremost is the acquisition of the precise waveshape of the primary field. The second is the robustness of the matching operation on noisy data. Linked to this second problem is the effect of having an inaccurate estimation of the primary field waveshape.

The COTRAN hardware records the waveshape of the transmitter current and rate of change of dipole moment. In principle, these waveshapes plus knowledge of the system transfer functions should permit very good estimation of the primary field waveshape. In practice, however, COTRAN data collected up until July of 1980 has not permitted utilization of the reference waveforms to estimate the primary waveshape. The reasons for this were two fold. First there was substantial differential drift between the four EM channels. This drift was far more severe than anticipated during hardware design and construction. Secondly, there was a minor defect in the A/D - HP2108 data transfer path which affected the reference channels only. As a result, the references were usable only at the 5000 to 10000 ppm level.

(a) Primary Field Waveform Estimation

In order to circumvent this problem, the received data from the bird coils were utilized to obtain estimates of the primary waveform. This problem is in some respects akin to the seismic wavelet estimation process in that the received signal is used to estimate the input into the system and the system response simultaneously. A wide variety of procedures were developed and tested for estimating the primary field. The details of the concepts tested would fill a book and will not be discussed at length here. The simplest procedure in the end was found to work the best for bulk data reduction and this procedure is described in the following.

The primary field waveform was estimated on a line-by-line basis. The basic principles are as follows. Following the formalism of section 2, the received signal at fid j has the form

$$R_j(t) = a_0^j P(t) + \sum_{n=1}^{N} a_n^j \int_0^\infty g_n(\beta) P(t-\beta) d\beta + e_j(t)$$

The objective is to estimate P(t) from $R_j(t)$ when $e_j(t)$, $g_n(t)$ and a_n are all unknown. This is obviously a difficult (impossible) problem. The approach taken to estimate P(t) is crude but relatively effective compared to the more elaborate schemes considered. Two primary field estimates Po(t) and $P_1(t)$ are computed for each survey line.

The first estimate of the primary field waveform is the mean of the received signal, namely,

$$P_o(t) = \langle R_j(t) \rangle$$

along a given survey line.

Upon the assumption that

$$\langle a_n^j \rangle = 0$$

and

$$\langle \varepsilon_j(t) \rangle = 0$$

one has

$$P_o(t) = \langle a_o^j \rangle \, P(t)$$

In practice, the average ground response is not zero and the assumption that $\langle a_n^j \rangle = 0$ is invalid. In highly resistive areas with few anomalies, however, this assumption is not totally unreasonable. The assumption that the noise averages to zero has been found to be a reasonable one in most instances.

In practice $P_o(t)$ is a reliable estimate of the primary field to better than 1 percent in most cases. $P_o(t)$ therefore provides a starting point for obtaining further primary fields estimates. The second primary field estimate $P_1(t)$ is obtained with the aid of Po(t). $P_1(t)$ is defined as

$$P_1(t) = \frac{\langle (R_j(t) - R_{j-1}(t)) \, (a_o^j - a_o^{j-1}) \rangle}{\langle (a_o^j - a_o^{j-1})^2 \rangle}$$

where a_0^j is amplitude coefficient which minimizes

$$R_j(t) - a_0^j \, P_o(t)$$

in a least squares sense. This operation estimates the primary field waveform by correlating differences between adjacent fids of data with the fluctuations in the estimated amplitude of the primary field. This estimator rejects ground response which is not correlated with primary field fluctuations. In general, the more receiver coil motion, the better estimator $P_1(t)$ becomes. Tests of this estimate indicate that it gives a very good representation of the primary field waveform. The procedure only becomes marginal in cases of very steady flight which yield very small variations in a_o.

The above developments for P_o and P_1 have been shown using the time domain waveform. The identical procedure can be carried out equally well in the frequency domain by Fourier transforming the time domain waveform as discussed in section 4.1. COTRAN data is generally handled in the time domain with the field playback system and in the frequency domain when data is processed on the large mainframe computer as the final data reduction is being carried out. The actual $P_1(t)$ estimate computed in the frequency domain during final data reduction is slightly different and somewhat simpler than the one described above. Instead of estimating a_o for each fid of data, the sign of the fundamental frequency, W_o , spectral component of the difference is used as the weighting factor.

Thus,

$$P_1'(W) = \frac{Q(W_o)}{P_o(W_o)} \; Q(W)$$

where

$$Q(W) = \left\langle \left(R_j(W) - R_{j-1}(W)\right)\left(\mathrm{sign}\left(R_j(W_o) - R_{j-1}(W_o)\right)\right) \right\rangle$$

The essential difference between P_1' estimated in this manner and P_1 estimated in the previous manner is that the P_1 estimater is more heavily biased towards the data with large excursions in the primary field. There is little to choose between the two results other than that the second form is computationally simpler to evaluate.

In practice, iterative procedures are used to estimate P_o and P_1. Initial estimates of P_o and P_1 are made. The residual error as discussed in the matching procedure is then estimated for each fid. Data records with large residual errors are then excluded on the next pass at estimating P_o and P_1 in order that very noisey or anomalous records do not contaminate P_o and P_1.

In order to provide a good stable primary estimate for each line of data even when primary field fluctuations are small, a linear combination of P_o and P_1 is used for P.

$$P = (1 - b)\ P_o + b\ P_1$$

where b is a parameter empirically related to the amount of primary field fluctuation along a line. For large motion induced primary field variations $b = 1$ whereas for small variations $b = 0$. For the data presented in this report, b is determined from the ratio $d = Q(w_o)/P_o(w_o)$ which reflects the magnitude of the signal fluctuations along the line being processed. The empirical formula for b which was employed is

$$\begin{aligned} b &= b_1\ d/do & d &< do \\ &= \sin^2 \alpha\ (d-d_2) & do &\leqslant d < d_1 \\ &= 1 & d &\geqslant d_1 \end{aligned}$$

where

$do = 0.015$
$d_1 = 0.0554$
$d_2 = 0.00459$
$b_1 = 0.1$
$\alpha = 30.91$

Thus, for average fluctuation levels greater than about 5% of the average primary field, $P = P_1$, whereas for small fluctuations some portion of Po is included in the estimate. In most instances, fluctuations from bird motion yield $b = 1$ and only on very stable lines with little turbulence is $b = 0$.

(b) Matching Stabilization

The general matching theory is outlined in section 4-1. In practice, the results of the matching process are frequently of poor quality because of imperfections in the estimation of the primary field waveform and because of finite noise levels in the data. These real data limitations lead to solutions which are not physically meaningful. In this section, two methods of constraining the matching process to give robust, physically meaningful results are outlined.

The general matching problem reduces to determining a set of amplitude coefficients a_i, $i = 1$ to N for the basis functions describing the ground response. In the unconstrained formulation presented in section 4-1, the a_i can take any value. Only a subset of all possible a_i solution vectors are physically plausible as a ground response. For the exponential models used here for example, a vector

$$a_i = (.01, .05, .001, .002, .005)$$

is a realistic solution in that it leads to a monotonically decreasing decay curve. On the other hand, a solution vector of the form

$$a_i = (0.1, -.01, .005, -\ .003, .002)$$

is not likely to be a true ground response since it leads to an oscillatory decay curve. With excellent data and a good primary waveform estimate, such oscillatory solutions are not observed. In order to accommodate situations where there are extra noise or imperfections in the primary waveform, the general matching process is augmented with constraints which bias against such oscillatory solutions.

Non-Linear Constraint

One manner in which the solution vector can be constrained is to require that an acceptable solution have coefficients of the same sign, namely,

$$a_i \geqslant 0 \quad i = 1 \text{ to } N$$

or

$$a_i \leqslant 0 \quad i = 1 \text{ to } N$$

This type of constraint results in a non-linear problem. The manner in which such solutions are obtained was developed by A. Loveless. The following discussion summarizes the algorithm employed to generate such solutiuons.

From section 4.1, the solution vector for the a_j satisfy the set of linear equations

$$C_{ij}\ a_j = D_j$$

with the corresponding solution

$$a_j = C_{ji}^{-1} \; D_i$$

and associated error energy E. The approach to obtaining solutions vectors with components of the same polarity is to solve the above set of equations with all permutations of the ground response coefficients constrained to zero and compute the associated error in each case. The set of all solution vectors is then searched for solutions with $a_i \geqslant 0$ or $a_i \leqslant 0$. The subset of satisfactory solutions are then weighted according to the inverse of their associated error and the final solution vector is the superposition of these weighted solutions.

To quantify this concept it is best to define the various solution vector permutations. First a solution vector F is defined as

$$\bar{a}_p = (a_D^p, a_1^p, a_2^p, \ldots \; a_N^p)$$

where p is an indication of which of the a_i i = 1 to N have been constrained to zero. For example, let p = o correspond to the case where no a_i are set to zero; p = 1 correspond to the case where a_1 = o; p = 2 correspond to the case where a_2 = 0; p = N + 1 correspond to the case $a_1 = a_2 = 0$ and so on. There N! possible solution vectors. The $\bar{a}_p$ satisfy the linear equation

$$C_{ij}^p \; a_j^p = D_i^p$$

where the appropriate rows and columns of the covariance matrix and the excitation vector relating to the a_j^p which are zero have been deleted. The corresponding error energy is E_p.

The matching program first computes a_o. If the solution is acceptable in the sense that all $a_i \leqslant 0$ or $a_i \geqslant 0$ for $i = 1$ to N, the solution is accepted and processing stops. If the solution is unacceptable, the program now passes through each of the p values which set only one of a_i to zero of which there are possible solutions. Should all the N solutions be acceptable, the final solution is defined as

$$\bar{a} = \sum\left(\frac{\bar{a}_p}{E_p}\right) \Big/ \sum\left(\frac{1}{E_p}\right)$$

If any of these N solutions are unacceptable, the ones which are unacceptable are continued into the higher order of setting additional coefficients to zero. This process continues until all possible solutions have been assessed. All acceptable solutions are then selected and the weighted average computed as above.

This algorithm has been found to work quite well and has been used extensively. Considerable analysis has still to be carried out in order to understand what biasing effect this type of solution has on the final solution. With good data and a good primary waveform estimate, the solution is the same as the unconstrained solution. In instances where there is a systematic error in the primary field waveform the outcome is less clear and becomes very dependent on the nature of the error in the primary field; this is a subject for future analysis.

Linear Constraint

An alternative and considerably simpler algorithm has been developed for quick analysis and is incorporated in the field replay system processing software. The approach is to solve the set of linear equations subject to the constraint that the magnitude of the solution vector is minimized in a manner which biases against oscillatory solutions. The manner in which this is done is to define a second quantity, Q, as

$$Q = \sum_{j=1}^{M} \sum_{i=1}^{128} w_i \left(a_j f_i^j\right)^2$$

Q is related to the energy of the secondary field. The secondary field energy is given by

$$B = \sum_{i=1}^{128} w_i \left(\sum_j a_j f_i^j\right)^2$$

$$= Q + C$$

where

$$C = \sum_j \sum_k a_j a_k \left(1 - \delta_{jk}\right)\left(\sum_i w_i f_i^j f_i^k\right)$$

The choice of Q as a quantity to minimize comes from the fact that Q is a positive quantity (i.e.; $Q > 0$). To put this in perspective, consider two solutions $\overline{a}_1$ and $\overline{a}_2$ which yield the same secondary field energy $B_1 = B_2$ but where a_1 has all secondary field coefficients of the same polarity while a_2 consists of coefficients of mixed polarity. The sum of the values of Q and C are equal but the Q and C values differ for the two solutions. Thus

$$Q_1 + C_1 = Q_2 + C_2$$

Examination of the C operation shows that $C_1 > C_2$ and therefore $Q_2 > Q_1$. Minimization of Q therefore biases against oscillatory solutions.

This constraint is applied by returning to the initial minimization step of the matching process. The set of normal equations were defined as

$$\frac{\partial E}{\partial a_j} = 0$$

The constrained solution is obtained by requiring that a linear combination of E and Q be a minimum, namely,

$$\frac{\partial}{\partial a_j} (E + \gamma Q)$$

where γ is a free parameter. The resulting set of normal equations take the form

$$C'_{ij} \, a'_j = D_i$$

where

$$C'_{ij} = C_{ij}(1 + \gamma(\delta_{ij} - \delta_{i,0}))$$

The degree of constraint is controlled by the magnitude of the free parameter γ . The larger the value of γ the greater the degree of constraint placed on the solution. The final solution is defined as

$$a_j = a_j'(1 + r(1 - \Delta_{j,0}))$$

The behaviour of the constrained solution is relatively easy to understand. The solution tends to bias energy into the shorter time constant part of the spectrum. Erroneous estimates of the primary field waveform shape affect the solution in a relatively predictable manner. Application of this constraint does stabilize the overall matching procedure and produces ground responses which are physically plausible. The choice of γ is arbitrary but optimal results have been obtained within the range 0.1 to 0.5.

To date the procedures for optimally constraining the COTRAN matching process have been developed on an intuitive basis. The need for constraint has arisen primarily because of limitations in the COTRAN data acquisition stage. Inadequate estimates of the primary waveform arising from the inability to use the transmitter reference signals forced the consideration of the constraint problem. Further assessment of this problem will be required as hardware improvements are installed in the system. A coherent study of the overall COTRAN matching procedure with a view to developing physically based constraints is essential.

4.5 Data Display

The COTRAN system collects a very large volume of data. Display of the data in a format which is convenient to the user and also contains all the COTRAN information is a difficult problem. The data display for bulk processing was chosen to be a set of "stacked" profiles. In this section, an overview of the manner in which the data is prepared for stacked profiles is presented. In order to put the following discussion in perspective, an example of a stacked profile section is shown in Fig. 4-1.

Starting from the top of the stacked profile section illustrated in Fig. 4-1, the top pair of traces are denoted RMSERR. These two traces give the RMS error for the vertical and horizontal signals at each fid after the data has been processed through the COTRAN matching algorithm. The RMS error is related to the total error energy E discussed in section 4.1 by the formula

$$\text{RMSERR} = \sqrt{\frac{E}{T}}$$

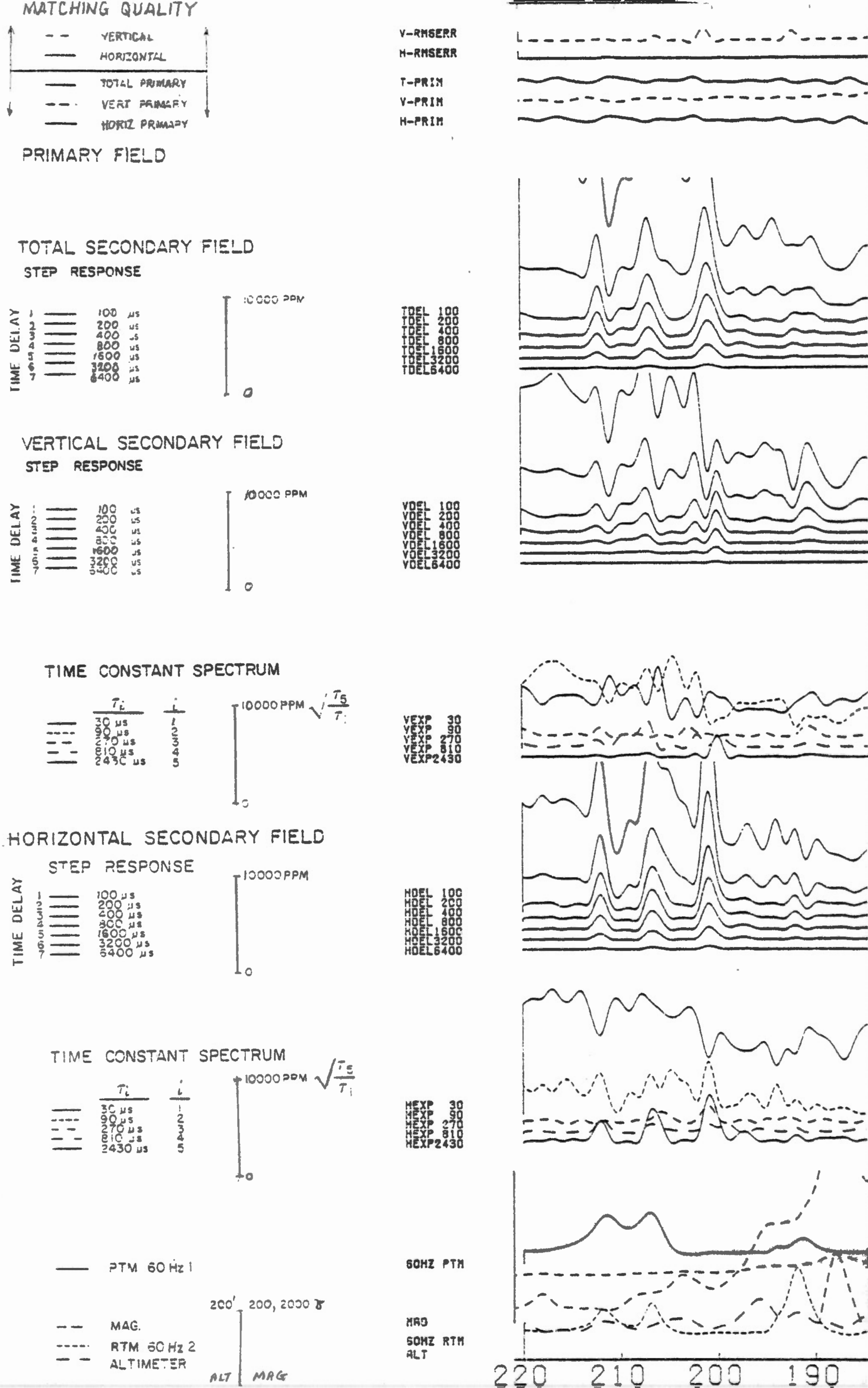
MATCHING QUALITY
VERTICAL
HORIZONTAL
TOTAL PRIMARY
VERT PRIMARY
HORIZ PRIMARY
PRIMARY FIELD
V-RMSERR
H-RMSERR
T-PRIM
V-PRIM
H-PRIM
TOTAL SECONDARY FIELD
STEP RESPONSE
TIME DELAY
1 100 µs
2 200 µs
3 400 µs
4 800 µs
5 1600 µs
6 3200 µs
7 6400 µs
10000 PPM
0
TDEL 100
TDEL 200
TDEL 400
TDEL 800
TDEL1600
TDEL3200
TDEL6400
VERTICAL SECONDARY FIELD
STEP RESPONSE
TIME DELAY
1 100 µs
2 200 µs
3 400 µs
4 800 µs
5 1600 µs
6 3200 µs
7 6400 µs
10000 PPM
0
VDEL 100
VDEL 200
VDEL 400
VDEL 800
VDEL1600
VDEL3200
VDEL6400
TIME CONSTANT SPECTRUM
T_i
i
30 µs 1
90 µs 2
270 µs 3
810 µs 4
2430 µs 5
10000 PPM $\sqrt{\frac{T_5}{T_i}}$
0
VEXP 30
VEXP 90
VEXP 270
VEXP 810
VEXP2430
HORIZONTAL SECONDARY FIELD
STEP RESPONSE
TIME DELAY
1 100 µs
2 200 µs
3 400 µs
4 800 µs
5 1600 µs
6 3200 µs
7 6400 µs
10000 PPM
0
HDEL 100
HDEL 200
HDEL 400
HDEL 800
HDEL1600
HDEL3200
HDEL6400
TIME CONSTANT SPECTRUM
T_i
i
30 µs 1
90 µs 2
270 µs 3
810 µs 4
2430 µs 5
10000 PPM $\sqrt{\frac{T_5}{T_i}}$
0
HEXP 30
HEXP 90
HEXP 270
HEXP 810
HEXP2430
PTM 60 Hz 1
MAG.
RTM 60 Hz 2
ALTIMETER
200' 200, 2000 γ
ALT
MAG
60HZ PTM
MAG
60HZ RTM
ALT
220
210
200
190

where T is the number of points on the waveform (i.e., 128). These two error channels are extremely diagnostic. Spurious anomalies generated by external noise of any sort are readily identified by abrupt changes in the ambient error amplitudes. Long term drifts in the system are reflected by long term variations in the error traces.

The next three traces are the amplitude of the primary field at the bird. The traces are the a_o coefficients which are derived in matching the horizontal and vertical received waveforms. Denoting the horizontal primary field amplitude as a_0^H and the vertical primary field amplitude as a_0^V, a third trace which is the "total" primary field a_0^T is generated from a_0^H and a_0^V as follows

$$a_0^T = \left({a_0^H}^2 + {a_0^V}^2 \right)^{1/2}$$

Since the coil system flies in a position where the transverse primary field is small, a_0^T is a reasonable approximation to the true total primary field. Yaw and roll of the coil system produce fluctuations in a_0^T while pitching motions leave a_0^T unchanged. Examination of relative variations of the three traces is indicative of bird and coil motion during flight.

The center part of the record consists of several groups of profiles labelled step response and time constant spectrum. The output of the matching process is two sets of 5 coefficients which characterize the ground response observed on the vertical and horizontal axis coils a_i^V and a_i^H $i = 1$ to 5. These coefficients are the amplitude coefficients for the exponential or loop response functions which are used to model the ground response. The time constant spectrum is the composite plot of each of these coefficients along a flight line. The group of five traces is referred to as the time constant spectrum since it represents the sampled version of the time constant spectrum outlined in section 4.2. Two time constant spectra are displayed; one for the vertical field and one for the horizontal field. This data display is very useful in that it permits a ready identification of the dominant time constant in an anomalous area.

For plotting purposes, different scales are required for the different time constant amplitude coefficients. In general $a_1 > a_2, > a_3 > a_4 > a_5$ where τ are in the sequence 30, 90, 270, 810, 3430 microseconds. A common convention was established for the plotting scales which worked reasonably well. The basic vertical scale is defined for the a_5 trace which corresponds to the longest (2430 microsecond) time constant as A ppm/inch. The vertical scale for all other a_i is defined as

$$A \sqrt{\frac{\tau_5}{\tau_i}} \quad \text{ppm/inch}$$

The result is that the scale for a_4 is $\sqrt{3}A$ ppm/inch, for a_3 is 3A ppm/inch, for a_2 is $3\sqrt{3}A$ ppm/inch and for a_1 is 9A ppm/inch.

In addition to displaying the secondary fields in a time-constant spectrum format, the step function response for both the horizontal and vertical ground response is also generated. The step function responses are

$$H(t) = \int_0^t g^H(\beta)\,d\beta = \sum_{i-1}^{5} a_i^H\, e^{-t/\tau_i}$$

$$v(t) = \int_0^t g^v(\beta)\,d\beta = \sum_{i-1}^{5} a_i^v\, e^{-t/\tau}$$

The step function response is just the integral of the impulse response function. The step function response was chosen for display rather than the decay portion of the impulse reponse because the step function response spans smaller dynamic range over a widely spaced delay time. The step function responses are displayed by sampling H(t) and v(t) at a set of geometrically spaced delay times and plotting the amplitude at each delay time as a trace. Data in this format permits comparison with other transient system responses. H and V are computed at delay times of 100, 200, 400, 800, 1600, 3200 and 6400 microseconds. The vertical and horizontal step function responses are displayed immediately above the corresponding time constant spectrum. In addition to the individual step function response, the "total" secondary field step response is also synthesized and plotted at the same set of delays. The "total" secondary field step response is defined as

$$T(t) = (V^2(t) + H^2(t)^{1/2}$$

It was felt that T(t) would provide a display which would reduce the bird motion modulation effect in areas of high ground conductivity.

The lower portion of the profiled data shows the magnetometer, altimeter and power line monitor signals. The mag data is plotted twice with a difference of a factor of 10 in the vertical scale. Two power line monitor signals are also plotted. The trace denoted RTM 60Hz 2 is the real time power line monitor signal digitized in flight. The trace denoted PTM 60Hz 1 is a second power line interference indicator extracted from the even harmonics of the horizontal and vertical EM data.

As a final point, all data traces are plotted using a cubic spline algorithm to generate smooth curves between the discrete sample points. The interpolated curve always passes directly through the data values. The splined curve gives the discrete data the same continuity as would be sketched by hand. The spline routine does generate some edge effects or ringing when extremely large jumps in data values are encountered. This is sometimes visible in the data at the edge of a big anomaly or at grossly noisy records. Further work into the optimal interpolating technique for the data is being carried out although the cubic spline is probably as good as can be achieved on a bulk processing basis.

4.6 DATA LAG CORRECTION

In order to accurately position the EM data on the flight path recovery, it is necessary to lead or lag the EM data. The manner in which the COTRAN data is shifted is outlined in the following.

The manner in which the INPUT system data is aligned with flight path recovery is to make the peak anomaly response from thin vertical conductors occur directly over the conductor. For a shallow target and the COTRAN coil system configuration, the maximum response is obtained on the horizontal axis receiving coil and occurs when the bird is located directly over the conductor. Since the flight path recovery camera is mounted in the aircraft, the EM response is displaced with respect to the aircraft location indicated by the film. In addition to displacement which is caused by bird-aircraft separation, most EM systems also have finite time lags in the electronics of the data collection system which cause even further anomaly displacement.

The lag in the COTRAN is primarily caused by the aircraft-bird separation. The COTRAN data is normally adjusted in a manner which causes the horizontal axis peak response for localized shallow conductors such as power lines to occur directly over the target position as picked from the flight path recovery film. For all COTRAN data collected prior to July 1980, a lag of one fiducial spacing was found to give optimal alignment of horizontal axis anomalies. This lag is automatically carried out when the data is plotted in profile form. In data listings, however, no such shifting is performed.

5. SURVEY AREA DESCRIPTION

The survey area was located just to the west of Wollaston Lake over an area which contains the Midwest Lake, the Asamera and the Canadian Occidental uranium deposits. The main test area was bounded by latitudes 58° 16'N and 58° ~~12~~ 20'N and longitudes 103° 50'W and 104° 07'W. Within this area, 32 east-west lines spaced 300 m apart were designated for survey flying. The lines are numbered 52 through 83 starting at the southern edge of the area. The line numbering system was previously defined by the high sensitivity mag and gradiometer survey conducted by the Geological Survey of Canada. The lines were approximately 17 km in length. A location map showing the survey area is given in Fig. 5.1.

In addition to the test survey grid, a long test line was flown into the deeper areas of the Athabasca Basin. The test line angled northwest across the survey grid and turned almost straight west over Midwest Lake. Midway out to Pasfield Lake, the line was swung southward to terminate at the southern edge of Pasfield Lake.

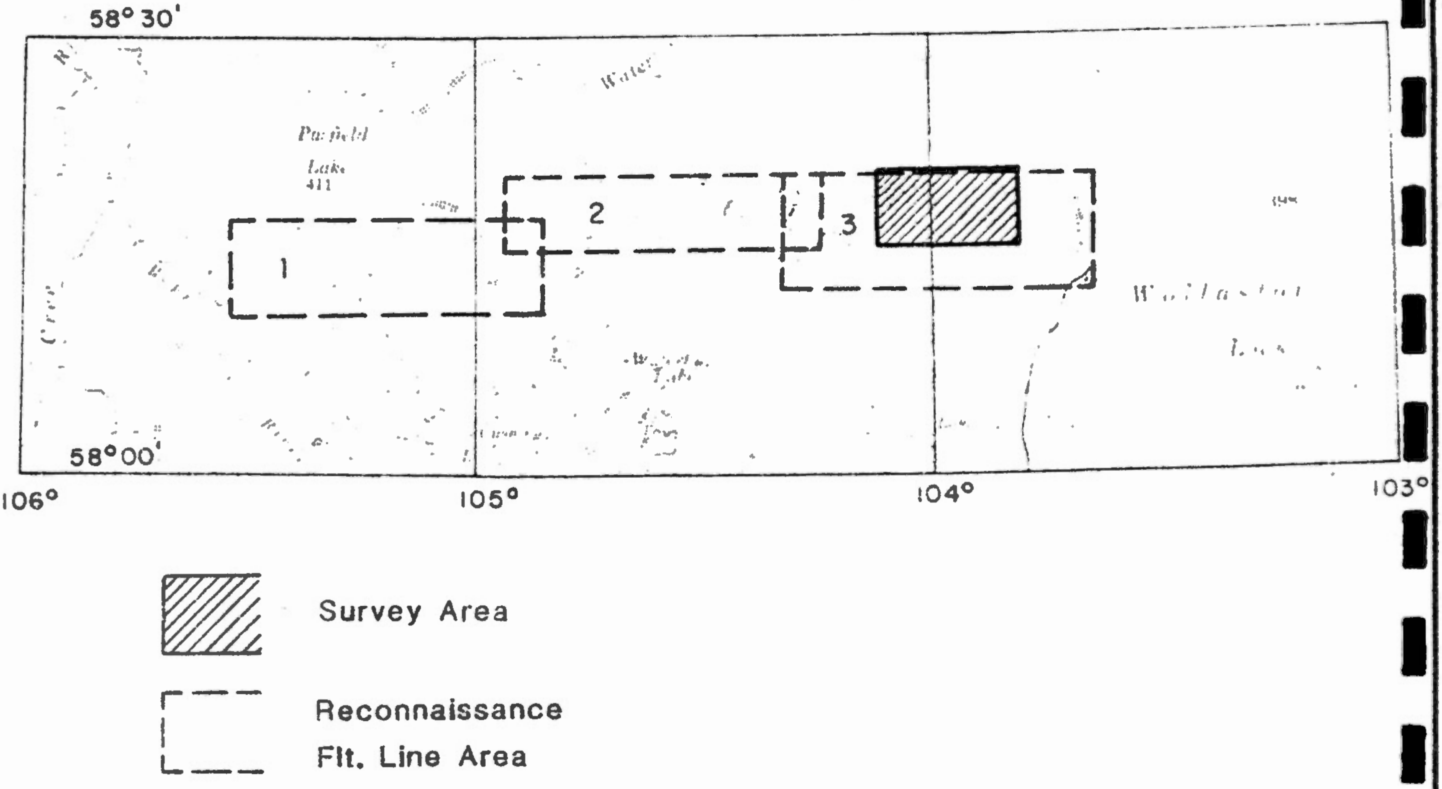

GEOLOGICAL SURVEY OF CANADA

COTRAN® AIRBORNE EM SURVEY

Athabasca Basin, Saskatchewan

TEST AREA LOCATION MAP

SCALE 1 : 1,000,000

FIGURE 5-1

6. SURVEY OPERATION DESCRIPTION

The survey was carried out in March 1980. The COTRAN aircraft was based in Toronto before system installation and mobilization to the survey area commenced. Mobilization to the survey area was initiated on March 12. Aircraft certification problems followed by poor weather conditions delayed the departure of the aircraft from the Toronto area until March 25. During the testing period in the Toronto area, the COTRAN system was given a thorough shakedown over Lake Ontario. In addition to testing the system, height fall-off tests were carried out over Lake Ontario. A brief test over a bedrock conductor was made at the Cavendish test site.

The base for survey operations was established at Lynn Lake, Manitoba. Lynn Lake was chosen as the operations base since it provided the best support facilities for the aircraft within a reasonable distance of the survey area.

The aircraft arrived in Lynn Lake late on March 26th. A preliminary test flight was carried out immediately after the aircraft's arrival in Lynn Lake. On March 27th, all the grid lines were flown. On March 28th, the long test line was flown and some of the grid lines were reflown. Demobilization commenced on March 29th.

Subsequent data reduction yielded 854 line km of useable data.

The COTRAN system operated quite well for the bulk of the survey. Since this was the initial survey with the system, the survey operation was not without its problems. A major problem cropped up during the first day of operations. Overheating in the COTRAN data A/D section upset the data transfer timing to the HP2108 computer. This problem was resolved in flight and the survey lines affected by the fault were reflown. While the problem was eliminated, a few bad fids of data still occurred on one or two lines which were not reflown. These bad records were not found until post flight data reduction. Only the horizontal axis data was affected.

In the second day of flying, problems were encountered with the coil suspension system in the bird. During the early part of the flight, the system worked fine. Later in the flight, the receiving coils began to bang against the suspension frame inside the bird. As a result, large noise transients were scattered throughout the data. Since much of the data most severely affected represented reflights of previously surveyed lines, only a small amount of useable data was contaminated with this problem.

The only other problem encountered was interference from a ground EM system; a large transmitter loop laid out on McClean Lake in the vicinity of the Canadian Occidental deposit. Portions of lines 53 through 59 in the area of the Canadian Occidental were contaminated with this interference.

7. FLIGHT PATH RECOVERY

The operational flying and initial flight path recovery (FPR) were made using a photo mosaic provided by Geological Survey. Upon returning to the office, the flight path recovery was reviewed and corrected. The final FPR was then transferred onto a 1:25,000 topographic map and printed on a stable base. The FPR for the survey grid appears on drawings 265-42-1,2,3, I. A separate, three section base at 1:50,000 was prepared for the long flight line at Pasfield Lake. The three section FPR is shown on drawing 265-42-R.

The fiducial numbers are labelled every 50 fids and the flight lines are ticked at every tenth fid. The FPR fids are signified by solid circles. For the survey grid, two series of fid numbers are used. For lines 52 through 66 fid numbers from 300 through 4439 are used. A system restart in flight caused the fid count to be reset to 1 between line 66 and 67. As a result, duplicate fid numbers are found on the FPR for the survey grid.

8. DISCUSSION OF SURVEY RESULTS

Analysis and discussion of the survey results can be far ranging in view of the fact that the data comes from a new system being flown in a rather unique geologic environment. In order to keep the analysis to the point, discussion is addressed to the data in three stages. In stage one, the data and how it is presented are discussed in order to make the reader familar with the data. In stage two, a general overview of the results is given from both a system performance viewpoint and from the geologic significance viewpoint. In stage three, individual details of the data are presented.

8.1 SYNOPSIS OF DATA PRESENTATION

The COTRAN data is presented in the stacked profile form discussed in Section 4 for primary analysis. The stacked profiles accompany this report as a separate volume. The volume contains a stacked profile for each flight line from 52 through 83 as well as the long test line to the west. While this data format is fine for examination of data on an individual line, it is very difficult to put the resulting data into perspective on a line-to-line basis.

In order to give a general overview of the data, a subset of the stacked profile data was selected for plottng in a plan format. The selected EM parameter is plotted on the stable base with the flight path recovery. The flight line forms the base line or zero level for the selected parameter. The parameter is then plotted along each flight line with the magnitude of the response being indicated by the distance from the plotted flight line. This forms an alternative stacked profile format which presents some of the data for all flight lines simultaneously in the correct spatial position.

Three sets of stacked flight line profiles were generated. On the first one, the vertical secondary field step response is plotted for delay times of 400 and 1600 microseconds. In the second plot, the horizontal secondary field step response is plotted for delay times of 400 and 1600 microseconds. In the third plot, the horizontal and vertical axis step response at a delay of 400 microseconds are combined to permit intercomparison of the vertical and horizontal response. These three sets of stacked flight line data accompany this report as drawings 265-42-1, 2 and 3.

In viewing the data, there are three problem areas which will immediately draw the eye. These are segments of data which have ground EM interference, A/D timing problems and receiving coil mechanical problems. The interference makes a hash of the COTRAN data on lines 52 through 59 in the vicinity of McClean Lake. The A/D problem generates occasional spikes in the horizontal axis data on lines 62 and 63. The coil suspension problems affect only data at higher fid numbers on the long line west. The data should be scanned several times in order that one knows what to expect when tracing anomalies into poor data areas.

8.2 GENERAL OVERVIEW OF THE DATA

The COTRAN data is difficult to assess from a quality point of view. Since this survey represented the first operational survey and the first time that the whole system package had been flown with all elements functional, there is no background data to compare against. The data certainly generates considerable interest. The dual axis receiving coil system opens up a new wealth of information. The data obtained with the vertical axis coil are quite exciting and far more informative than was originally anticipated.

The following items are the most characteristic features of the data.

a) In general, the vertical axis coil data were far more diagnostic than the horizontal axis coil data.

b) The vertical axis coil anomalies are generally bigger than the horizontal axis coil anomalies. The vertical axis data also shows much greater line to line correlation.

c) All the major anomalies in the survey area tend to strike southwest and northeast. The only exception to this occurs in the northeastern quadrant of the survey area. This area is full of anomalies which seem to be almost continuous. In the early phase of data examination, it was felt that the continuous anomaly was caused by a conductor with a strike parallel to the flight direction. While this would be plausible for a single line anomaly, it does not explain the general continuation of such features over several adjacent lines which the stacked survey line data clearly illustrates.

d) From an EM response point of view, the survey area could be divided cleanly into two separate parts. A line drawn in a northwesterly direction from fid 650 on line 52 through fid 2900 on line 83 divides the area as far as the EM response is concerned. All the major anomalies are located to the east of this separating or dividing line. There are two possible explanations for this behaviour. The first is that the major anomalies are located in the basement and are covered by an increasing thickness of sandstone cover. The dividing line would, therefore, suggest that this is the demarcation line where the sandstone thickens to a point where many of the EM responses are too weak to be detectable. A major change in the subsurface geology is also an alternative explanation for this sudden abrupt change in EM response character.

e) An overall perspective of the EM response of the area is obtained best by examination of the stacked flight line profile data for the vertical axis coil. This data gives the best line to line correlation and therefore continuity of anomalies from line to line. The stacked flight line profiles of the horizontal axis data are not nearly as useful. When used in conjunction with the vertical axis coil data, however, the horizontal axis coil data is quite often diagnostic of the shape of the conductor.

f) The anomalies in the area all tend to be very broad. Anomaly widths of up to 2 to 3 km are not uncommon. Within the broad conductive zones the time constants of ground response can vary considerably. In general, the broad anomaly is usually characterized predominantly by a relatively short time constant response. Within this broad zone of short time constant response, 1, 2 or even 3 longer time constant zones will appear. In general, trying to characterize the ground response in terms of discrete conductors is quite often unrealistic.

g) The EM response seems to show a very strong correlation with the general character of the magnetic response over the area. The east-west demarcation line is also a significant feature on the airborne gradiometer data collected by the Geological Survey of Canada. Many of the anomalies in the eastern half of the map sheet have a direct magnetic expression. EM conductors frequently appear to lie on the flanks or in the bottom magnetic lows.

h) Aside from the problems with the data regarding noise and external interference, the overall quality of the results is quite good. In viewing all the data, some care must be taken in accepting the actual decomposition into the time constant spectra at face value. As mentioned earlier in this report, system drifts and changes in the reference can cause some bias in the time constant spectra. A systematic error in the shape of the primary field waveform often results in a systematic shift of the step response as observed in the horizontal axis receiving coil. The responses appear as if somebody has shifted the DC level for the whole trace. If there has been a systematic change in the primary field waveform, this can usually be detected by looking at the RMS ERR trace. This trace will usually show a characteristic increase or decrease in the quality of the match. Line 68 is a particularly good example of the behaviour of the horizontal axis coil when a systematic error creeps into the primary field waveshape. An error in the primary field waveshape on the vertical axis coil leads to very noisy and chattery data. An example of this type of problem is shown on line 73 for the vertical axis coil.

8.3 DETAILED ANOMALY DISCUSSION

No attempt is made in this section to discuss all of the anomalous features in detail. What has been done is that the major EM anomalies have been identified and their general trend is followed from line to line. A detailed interpretation of individual features is best carried out in conjunction with people who know the detailed geology in the area. As a result, anomaly discussions in this section are constrained to primarily deal with the general features of the anomaly shape and characteristics

In order to provide some indication as to the nature of the source of anomalies, the relative vertical and horizontal axis responses for a flat lying and vertical ribbon conductor are sketched in Fig. 8-1. No claim is made that these shapes are perfectly correct for either of the models. What has been done here is to put together the general nature of the anomaly which would appear over either of the targets. The main feature to note is the vertical axis coil has a crossover over the vertical ribbon and the horizontal axis coil has a maximum response directly over the vertical ribbon. Exactly the opposite is the case for the flat lying ribbon. For the flat lying ribbon, the vertical axis response is a maximum directly over the flat lying ribbon while the horizontal axis coil peaks at the front edge of the ribbon. While this tends to be an over simplified discussion, judicious use of these curves is very helpful in understanding the general character of the anomaly observed in the stacked profile data. The major point to note from these anomaly shapes is that a vertical ribbon flown in alternate flight directions will give a maximum on the horizontal axis coil which is continuous from line to line. The vertical axis coil on the other hand will show staggers as back and forth or herringbone effects as the flight lines alternate in direction. The exact reverse is true for the flat lying ribbon conductor; in this case, line to line correlation should be seen primarily on a vertical axis coil and staggering of anomalies should be observed on the horizontal axis coil.

Another general point to be noted before going into discussion of detailed features is the relative magnitude of vertical and the horizontal axis responses from flat lying conductors. In general, the deeper the flat lying target, the more vertical the secondary response becomes. As a result, seeing an anomaly which is primarily on the vertical axis coil and only weakly

Schematic Illustration of Anomaly Shape for Vertical & Horizontal Ribbon Conductors

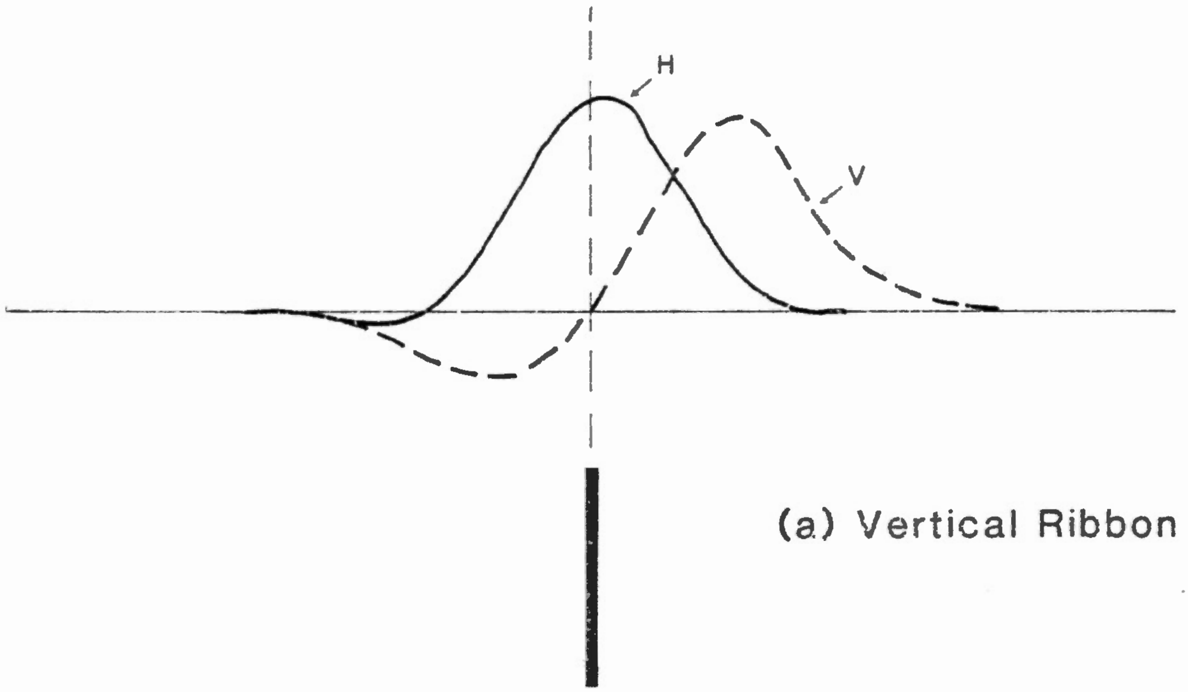

(a) Vertical Ribbon

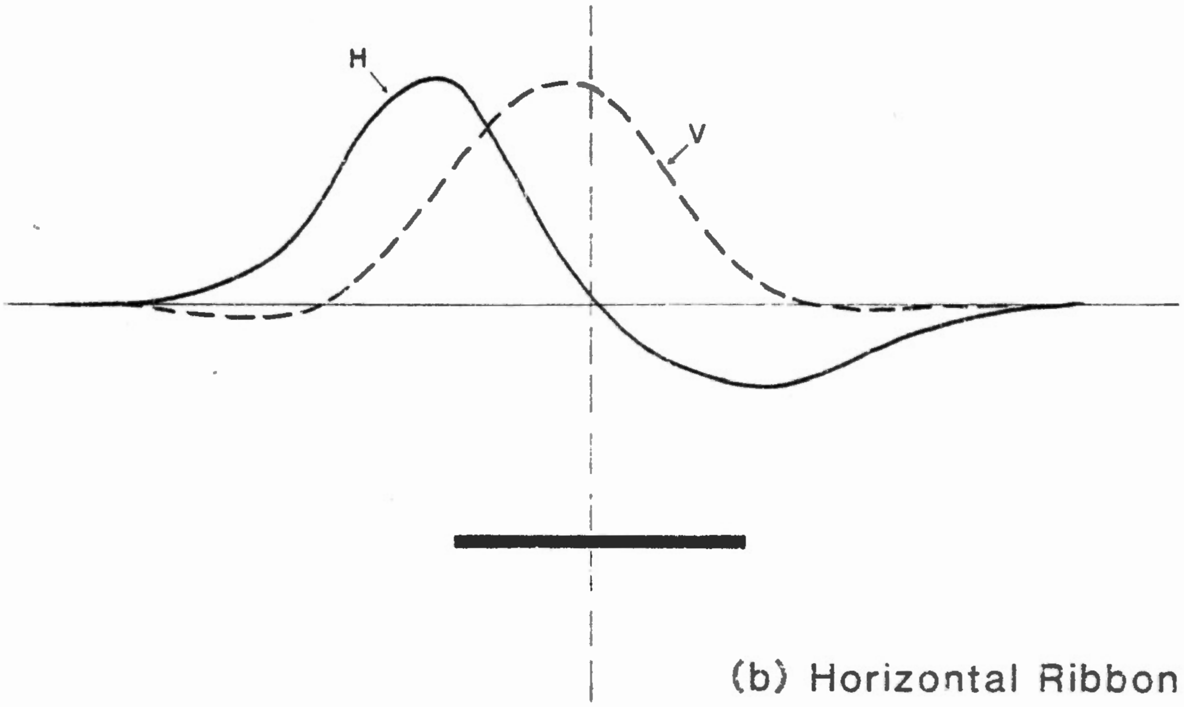

(b) Horizontal Ribbon

FIG. 8-1

observed on the horizontal axis coil, is a general indication that the response is coming from a flat lying conductor at considerable depth. One need only treat the conductive half space model using simple image theory to see that this is the case. This point is particularly noteworthy for the COTRAN data observed in the Athabasca Basin. Quite often the vertical axis anomaly is substantially larger than the horizontal axis anomaly. If the response were overburden response one would tend to suspect roughly equivalent magnitudes for the horizontal and vertical axis responses.

For the purposes of detailed discussion, major features in the survey area have been identified as alphabetically designated zones. These zones are designated A through H. In some instances, these zones correspond to a distinct anomaly; in other instances, these zones indicate a broad area of anomalous behaviour.

Zone A

Zone A is actually a distinct conductive feature which has the most extensive strike extent of any anomaly in the area. Zone A runs down the very eastern edge of the survey area. Some of the survey lines are extended to the east in order to track this anomaly. This anomaly follows a major structural feature indicated by aeromagnetic surveys carried out in the area. The anomaly is continuous running to the southwest until lines 56 and 57. At this point, the anomaly is abruptly terminated and appears to be shifted to the eastward and continued on to the south. Two separate conductors designated A' and A'' are identified as continuation of Zone A. It is conjectured that a major fault cuts this feature and has shifted it to the southeast.

The source of this anomaly is thought to be fairly shallow. The reason for this is that both the vertical and horizontal responses are relatively large in amplitude. The shallow source is consistent with the fact that the sandstone formation is thinning rapidly to the eastward. At the very southern end of A' and A'', the conductor seems to be a very broad conductor in terms of the short time constant responses but segregated into two distinct zones in terms of the long time constant response.

<u>Zone B</u>

Zone B represents a major conductive feature which runs down the eastern side of Torwalt Lake. The anomaly generally tends to have a fairly sharp western edge then tail out gradually to the eastward. This is suggestive of a conductor which is dipping at a very shallow angle to the eastward. This major feature is most apparent in the short time constant response. The long time constant response tends to show zoning within the conductor itself. The conductor extends northward from the top of McClean Lake and terminates abruptly northeast of Torwalt Lake. The southern end of the anomaly is lost in the zone of interference caused by the ground EM system operating in the area. As a result, it is difficult to infer exactly where the anomaly goes at the southern end. It is certain that the anomaly does not terminate. It can either swing slightly towards the east and cross through McClean Lake-Candy Lake area or it could swing slightly southwest and go through Zone B'.

<u>Zone B'</u>

The area designated Zone B' appears to merge with the southern end of Zone B. As a result, it is tentatively connected to Zone B to form a continuous anomalous area. Zone B' tends to show very broad anomalies. While this may be partially due to the fact that most of the flying is parallel to the trend of the conductor, this is not the total explanation of the width. The anomaly source itself must be a very broad conductive zone.

Since Zone B also lies almost straight down the extension of Zone C, there is also the possibility that Zone B could be a continuation of Zone C which is discussed next. From the general behaviour of the response, however, it would be more likely that Zone B' links into Zone B and the anomalous area under Zone G which will be discussed later.

Zone C

Zone C contains a major conductive anomaly which runs down the western flank of Torwalt Lake. The northern end of the conductor merges with the scrambled Zone H which is discussed later. At the southern end, the anomaly terminates abruptly just south of Torwalt Lake. The anomaly response tends to peter out both north and south from lines 67 and 68. The anomaly is strongest along line 67 and 68 and appears to be extended to the westward. The westward extension may represent just a broadening of the conductive zone or it may represent a discrete conductor lying to the west of Zone C. The zone seems to be continuous over a wide area on the short time constant responses but tends to be more segregated when the longer time constant responses are examined.

Zone D

Zone D is not so much a particular anomaly but rather a demarcation line between the eastern anomalous area and the western quiet area of the survey grid. The northern end of Zone D is the location of the Asamera Dawn Lake deposit. The deposit itself is located roughly on Zone D at lines 81 and 82.

At the northern end of Zone D, D is not a distinct conductor but rather the edge of the broadly anomalous Zone H, to be discussed later. Tracking the anomaly or anomalous zone to the southwest, one finds that the anomalies along D tend to fade out. While the anomalous area tends to fade, it does not totally disappear and it seems to be patchy but continuous and Zones D' and D'' would appear to be along the extension of the strike of Zone D.

It has been suggested that the variation of anomalous response along the line designated D could be attributed to variations in the thickness of the sandstone cover. In areas of thick sandstone cover, the anomaly weakens and almost disappears. In areas where the sandstone thins and the basement comes closer to surface, the anomaly responses pick up. Again, this is very conjectural and only more detailed knowledge of the geology will confirm any such conjecture.

Zone D'

Zone D' is thought to be a continuation of Zone D. This is speculative, however, since the trend of this feature tends to be almost straight north which is not consistent with the trend in Zone D. In general, Zone D' shows a very broad short time constant response which is almost elliptical in shape when looked at in plan view. Zone D' has a localized central long time constant response which is most evident on line 58 around fid 1604. The response tends towards shorter time constants as one moves away from this central core in any direction.

Zone D''

Zone D'' is again conjectured to be on the continuation of Zone D. The majority of the anomaly occurs over a lake. The horizontal and vertical axis responses are both fairly large. This behaviour would suggest the source could be lake bottom sediments. The only possible argument against this is that the anomaly carries onto the shore northeast of the lake and trends towards Zone D' and D.

Zone D, D' and D'' all tend to be lined along a distinct boundary indicated by the aeromagnetic data. As such, the Zone D and its continuation are related to a major change in subsurface conditions. One possibility is that this is a major fault zone and the sandstone thickens substantially to the west of this line. An alternate possibility is that this line demarks a major change in the composition of the basement material.

Zone E

Zone E is a weak anomaly which trends northwest-southeast. It is observed primarily on the vertical axis data. The anomaly itself is not continuous over all lines in which it is indicated on the map. The anomaly is missing on some lines and continuity has been ascribed by conjecture and not on the basis of fact. This anomaly has been identified primarily because it is one of the few features which appear west of the demarcation line D.

Zone F

Zone F is over the Midwest Lake deposit. The anomaly itself is weak and not very convincing in the profile data. Extensive examination of the raw data shows that this area is indeed anomalous and further data processing might enhance the response in this area. In general, line by line processing tends to bias the data somewhat and suppress very weak anomalies. While this is not a major problem, it is something which will have to be addressed in the future if the reference problem for the COTRAN system is not resolved.

In order to illustrate the response over Midwest Lake, a section of what are denoted as wiggle traces is presented in Fig. 8-3. The wiggle traces represent the EM response waveform at each fid after the primary field has been removed with the least squares matching procedure. In the plot, each fid of data is represented as traces plotted horizontally across the page. The EM response amplitude is vertical. Each wiggle trace is the average half cycle (5.5 milliseconds) COTRAN waveform observed at each fid. As such, each wiggle trace is the average of 252 successive half cycle of data. One can see that both the vertical and the horizontal responses show characteristic signatures which correspond to those postulated in the earlier sections of this report.

Zone G

Zone G is the area over McClean Lake and Candy Lake where the Canadian Occidental deposit is located. This zone is quite anomalous and appears that it could be an extension of Zone B. It is very difficult to analyse the information shown in the stacked profile data or on the stacked flight line map because of the interference caused by the ground EM system operating in the area. Extensive examination of the wiggle trace data associated with this area shows that the area is indeed anomalous. Part of the EM response might be attributable to the inductive response of the ground loop. In order to get a rough idea what is a happening in the area, an average line can be drawn through the noisy traces to give a crude indication of the anomalous response.

Zone G is hatched on the map in order to indicate the data is subject to interference from an external source.

RESIDUAL COTRAN WAVEFORMS
OVER MIDWEST LAKE
Line 67 E

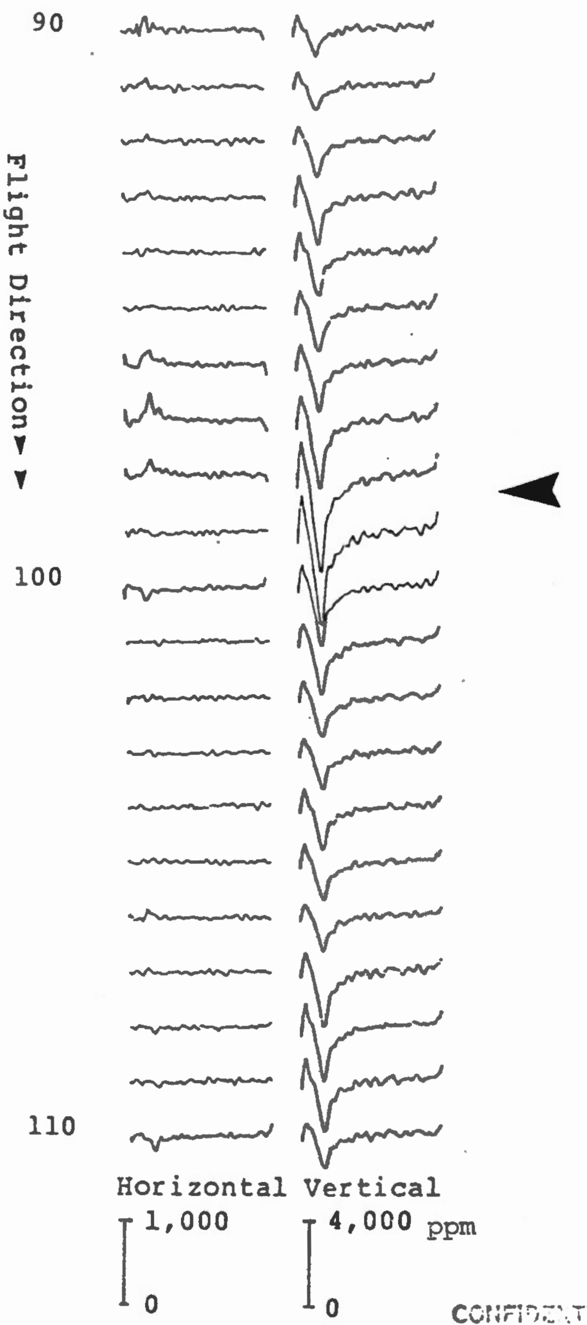

FIG. 8-2

Zone H

Zone H encompasses the northeastern corner of the survey area. This area is rather a chaotic mess. The whole area appears to be conductive. While there is some line to line correlation, higher responses occur in patchy areas. No strike or trend can be ascribed to the anomalies. The area is bounded to the west by Zone D and forms a continuation of Zone C. In general, short time constant responses persist over the whole area with patches of long time constant response dispersed throughout. It has proved very difficult to try and subdivide this area into discrete conductors.

An explanation for this behaviour is a major zone of flat lying conductive material. The longer time constant responses may be attributed to zones where this material thickens and thins. An alternate explanation of the longer time constant responses is to associate these zones with vertical conductors which may underlie this flat lying zone of conductive material.

8.4 POSSIBLE ANOMALY SOURCE MECHANISM

Since the vertical axis response dominates in most anomalous areas, a model which might be consistent with the observed data is shown in Fig. 8-3. The model consists of a resistive sandstone cover overlying a flat lying conductive regolith. This flat lying conductive zone will vary in thickness and lateral extent. The conductivity of this zone may also vary substantially depending on the alteration in the area. This flat lying conductive zone is underlain by steeply dipping graphitic conductors. Such a model is the simplest one which can be postulated to explain the types of responses observed with the COTRAN system. The persistent short time constant responses would be attributed to the flat lying conductive regolith. Zones of thickening of the regolith or underlying vertical conductors could give rise to the localized zones of longer time constant response.

The above model is very crude and simplistic but it does explain the major features of the responses observed. Only more detailed interpretation in conjunction with geological control information will really resolve the exact nature of the source of the EM responses.

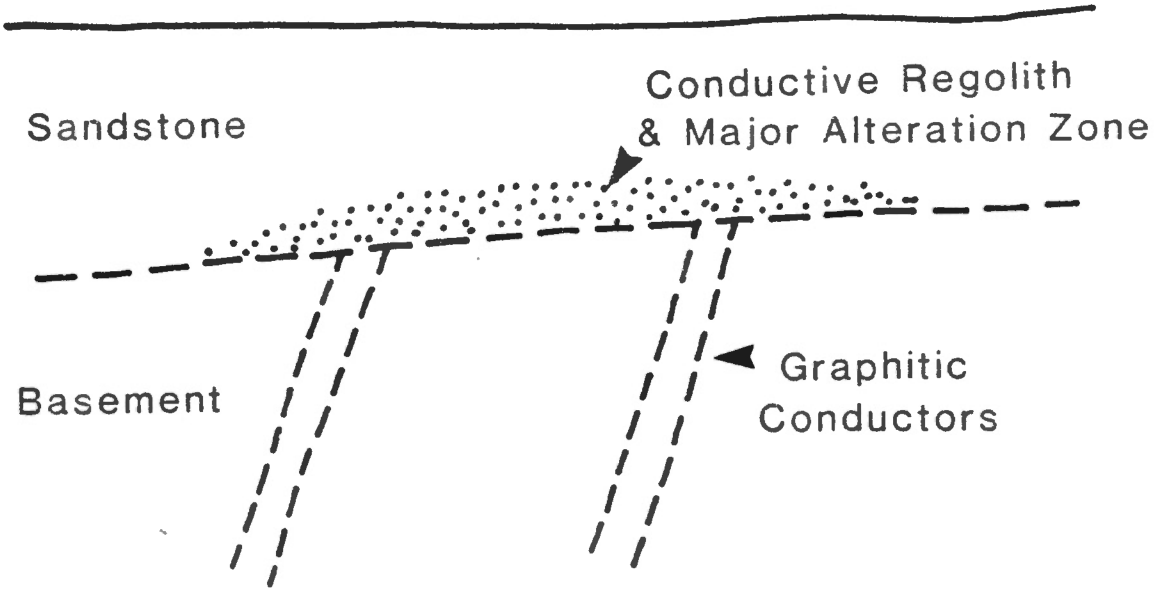
Conductive Regolith
& Major Alteration Zone
Sandstone
Basement
Graphitic
Conductors

Fig. 8-3

9. SUMMARY AND DISCUSSION

The COTRAN survey carried out for the Geological Survey in the Athabasca Basin has proven to be a very successful operation. As a first survey for the COTRAN system, the results are quite impressive. On-going developments with the system should remove some of the problems which were encountered during this survey. Even though some instrumentation difficulties caused problems in the analysis of the data, the data is of relatively good quality and sheds new light on the overall Athabasca Basin picture.

This report has attempted to give a general overview of the COTRAN system and to give a detailed discussion of the data collected during the survey. The data warrants considerably more analysis and work should be carried out in this regard by the Geological Survey in conjunction with the people who own property in the survey area. For even more detailed diagnostic interpretations, detailed wiggle section format records could be generated in order to help with the interpretation. A great deal of time has not been expended on this type of data display at this juncture in time. This is an area which could be fruitfully pursued should such detailed information be felt to enhance the interpretation.

In conclusion, it is important to note that the COTRAN system represents a new evolution in airborne EM. The whole concept of totally digital airborne EM is a revolution to the general business community. To carry out EM in a totally digital manner, there are many pitfalls and difficulties which are encountered. This survey shows that it is possible to carry out such work and do it with reasonable reliability. As the system developments progress, the efficiency and the utility of the data will improve steadily. The results of this survey should really be viewed as the start of a revolution. Airborne EM will jump into the digital era very quickly and more sophistication will then enter the EM business in the near future.

APPENDIX A

COTRAN DATA TAPE FORMAT

This section describes the format of COTRAN raw data as it is put on digital magnetic tape during data acquisition. All COTRAN data tapes are 9 - track and recorded at a density of 800 PBI. Each tape has a standard format in which a directory file is written at the beginning of the tape. The directory contains all information relevant to the flight on which the tape was recorded and a flight log breaking down the actual contents of data on the tape. The directory record has a length of 960 bytes. The format of the directory record is given in Table A-1.

For housekeeping purposes, the directory file is actually within the tape twice and is followed by two EOF or tape marks which are separated by a short section of random garbage. The COTRAN data commences after the second tape file mark. Each system cycle generates a tape record with a unique Fid number. The data records are written sequentially as a single tape file until the end of data acquisition for the tape. At the end of data acquisition, a double file mark is written on the tape to indicate the end of the data for the tape. The format for each data record is outlined in Table A-2.

In general, more than one data tape is used during a flight. Barring system failures, each tape is assigned a sequence number by the HP2108 computer which is written in the tape directory. The fid numbers continue to increase and tapes recorded adjacent in time have contiguous fid number sequences. In the initial stages of COTRAN development in 1980, the system occasionally failed to increment the tape sequence number. In addition, the flight log portion of the directory was occasionally left blank. The housekeeping software in this area was subsequently modified in October 1980 and such problems have been eliminated.

TABLE A-1

COTRAN MAG TAPE

DIRECTORY SPECIFICATIONS

Length 480 Integer x 2 Words or 960 Bytes

Word	Byte	Identity	Contents/Description
1-2	1-4	IFLHT(2)	4 character flight designation
3-6	5-12	ITAPL(4)	8 character tape label
7	13-14	ITAPE	Tape sequence number
8	15-16	IYR	year 2 characters
9	17-18	IMN	month 2 characters
10	19-20	IDAY	day 2 characters
11	21-22	1HR	hour 2 characters
12	23-24	IMIN	minute 2 characters
13	25-26	ISEC	second 2 characters
14-16	27-32	IJOB(3)	6 character job name
17-21	33-42	IBASE(5)	10 characters designating flying base
22-26	43-52	IAREA(5)	10 characters designating flying area
27-28	53-56	LSPC(2)	line space 4 characters
29-30	57-60	IHGHT(2)	flying height of aircraft 4 characters

Word	Byte	Identity	Contents/Description
31-33	61-66	ICRFT(3)	6 character aircraft designation
34-36	67-72	IFREQ(3)	6 character fundamental frequency
37-42	73-84	ICHEF(6)	12 character name of crew chief
43-48	85-96	IPILT(6)	12 character name of pilot
49-54	97-108	INAV(6)	12 character name of navigator
55-60	109-120	IOPTR(6)	12 character name of operator

Each tape directory contains a flight log of 20 individual flight sections/tape. The number of selections filled with information is determined by the number times data acquisition is started and stopped during the use of a tape.

61-180		ILINE(20,6)	20-12 character flight line names
181-220		IFIDR(20,2)	start and end fid numbers for 20 flight lines
221-480		IRMRK(20,13)	20 - 26 character comments for individual flight lines

NOTE: Characters are Asc II character code. (both upper and lower case + numerics)

Table A-2

COTRAN MAG TAPE

DATA RECORD SPECIFICATIONS

Length 3085 Integer x 2 Words or 6170 Bytes

Word	Identity	Content
1	IFID	Record fiducial number
2	MFID	Manual fid counter
3	IPNTR	Section of flight log in directory which relates to this record
4-8	IAI(5)	5 integer x 2 words containing low speed analog signals (2 - 60 Hz 1 - Alt 3,4,5 - Fluxgate)
9-10	IDI(2)	Digital data from low speed RTP. Contains mag in BCD plus manual fiducial flag
11-12	MAG(1)	Contains magnetic field MAG(1) - mag field/10000 MAG(2) - mag field mod 10000
13	IASC	Pointer indicates which EM channel is multiplexed through A/D channel 1 for the current record, currently disabled.
14-1037	IG (4,128)	Array containing 4 EM waveforms in 32 bit integer format. (Integer x 4).

Word	Identity	Content
1038- 2061	E(4,128)	Array containing 4 EM waveform half cycle sums in 32 bit integer format
2062- 3085	H(4,128)	Array containing 4 EM waveform half cycle differences in 32 bit integer format

ATHABASCA FLIGHT LOG - FLIGHT 1 - 27/3/80

LINE	HEIGHT	FID START	FID STOP	TAPE	COMMENTS
		1	132	BRL323	Hi S & L - Mag adj
		133	363	BRL323	Hi S & L - swoop
		354	384	BRL323	Test replay
52W	450	385	591	BRL323	SL 404 Turam 460
53E	450	592	762	BRL323	SL 605 Turam 711-730
54W	450	763	953	BRL323	SL 780 Turam 812-830
55E	450	954	1132	BRL323	SL 920 Turam 1080 peak 1093-1098
56W	450	1133	1318	BRL323	Turam 1180
57E	450	1319	1472	BRL333	Turam 1425-14
58W	450	1473	1671	BRL333	SL 1490 Turam 1520-1540
59E	450	1672	1812	BRL333	T-1770 1780
60W	450	1813	1997	BRL333	SL 1825 T - 1860-1870
61E	450	1998	2170	BRL333	T - 2130-2150
62W	450	2174	2355	BRL333	T - 2230-2240
63E	450	2356		BRL333	T - 2480-2510
64W	450		2758	BRL333	T - 2625-2650
65E	450	2759		BRL338	
66W	450			BRL338	
67E	450	3080		BRL338	
			3611	BRL338	System debug

APPENDIX B

Flight Log

The following table gives an account of the in-flight commentary. This information is appended to the report to assure that a copy of the first hand notes is always available should someone wish to re-examine the raw data at some later time.

ATHABASCA FLIGHT LOG - FLIGHT 1 - 27/3/80

LINE	HEIGHT	FID START	FID STOP	TAPE	COMMENTS
		1	132	BRL323	Hi S & L - Mag adj
		133	363	BRL323	Hi S & L - swoop
		354	384	BRL323	Test replay
52W	450	385	591	BRL323	SL 404 Turam 460
53E	450	592	762	BRL323	SL 605 Turam 711-730
54W	450	763	953	BRL323	SL 780 Turam 812-830
55E	450	954	1132	BRL323	SL 920 Turam 1080 peak 1093-1098
56W	450	1133	1318	BRL323	Turam 1180
57E	450	1319	1472	BRL333	Turam 1425-14
58W	450	1473	1671	BRL333	SL 1490 Turam 1520-1540
59E	450	1672	1812	BRL333	T-1770 1780
60W	450	1813	1997	BRL333	SL 1825 T - 1860-1870
61E	450	1998	2170	BRL333	T - 2130-2150
62W	450	2174	2355	BRL333	T - 2230-2240
63E	450	2356		BRL333	T - 2480-2510
64W	450		2758	BRL333	T - 2625-2650
65E	450	2759		BRL338	
66W	450			BRL338	
67E	450	3080		BRL338	
			3611	BRL338	System debug

LINE	HEIGHT	FID START	FID STOP	TAPE	COMMENTS
62W	450	3611	3801	BRL339	
63E	450	3802	3959	BRL329	
64W	450	3960	4134	BRL329	Minor A/D (gold?)
65E	450	4135	4278	BRL329	
66W	450	4279	4449	BRL329	

System drop - change to new tape - System Restart

LLB - 1-37

LINE	HEIGHT	FID START	FID STOP	TAPE	COMMENTS
67E	450	38	203	BRL342	
68W	450	204	376	BRL342	
69E	450	377	536	BRL342	
70W	450	537	722	BRL342	
71E	450	723	879	BRL342	
72W	450	880	1069	BRL342	
73E	450	1070		BRL342	Nav. refly
73W	450		1393	BRL342	
74E	450	1394	1543	BRL342	
76W	450	1544	1720	BRL309	
76E	450	1721	1871	BRL309	
77W	450	1872	2041	BRL309	
78E	450	2042	2190	BRL309	
79W	450	2191	2367	BRL309	
80E	450	2368	2508	BRL309	
81W	450	2509	2671	BRL309	
82E	450	2672	2819	BRL309	
83W	450	2820	2985	BRL309	
CLIMB		2986	3185	BRL309	

ATHABASCA FLIGHT 2 LOG - 28/3/80

LINE	HEIGHT	SOL	EOL	TAPE	COMMENTS
		1	108	BRL310	Hi background 4000'
		109	421	BRL310	Hi test and decent
Test Line West	450	422	549	BRL310	SL 481 Scrub
Test Line West	450	550	1335	BRL310	SL 569 Coil banging in turb
Test Line East	600	1366	2065	BRL346	
64W	450	2079	2226	BRL346	
65E	450	2227	2376	BRL346	
66W	450	2388	2562	BRL346	
67E	450	2563	2640	BRL346	Coil hit turbulence
68W	450	2650	2748	BRL346	Coil hit turbulence
69E	450	2750	2807	BRL346	Coil hit turbulence
70W	450	2808	2952	BRL346	Scrub 2817 restart 2877
71E	450	2953	3003	BRL346	Scrub 2817 restart 2877

TESTING

ATHABASCA FLIGHT 2B LOG - 28/3/80

LINE	HEIGHT	SOL	EOL	TAPE	COMMENTS
		Speed Tests			
	4000'	18	87	BRL320	100 knots
	4000'	107	157	BRL320	110 knots
	4000'	187	247	BRL320	120 knots
	4000'	257	317	BRL320	130 knots
	4000'	337	377	BRL320	Circle CCW
	4000'	387	437	BRL320	Circle CW
	4000'	587	607	BRL320	Pitch - Tx off - Sample clock off
	4000'	667	697	BRL320	Pitch - Tx off
Altimeter Calibration					
	1500'	698	737	BRL320	S & L
	1000'	777	807	BRL320	S & L
	750'	837	867	BRL320	S & L
	500'	877	917	BRL320	S & L
	450'	927	1027	BRL320	S & L